# SOFTWARE-DEFINED MOBILITY MANAGEMENT AND BASE STATION CONTROL FOR GREEN CELLULAR NETWORKS

A DISSERTATION
IN
Telecommunications and Computer Networking
and
Electrical and Computer Engineering

Presented to the Faculty of the University

of Missouri - Kansas City in Partial Fulfillment of

the Requirements for the Degree

DOCTOR OF PHILOSOPHY

by
SUNAE SHIN

M.S., South Dakota State University, Brookings, SD, USA, 2007
B.E., Kyung Hee University, Seoul, South Korea, 2005

Kansas City, Missouri
2015

SOFTWARE-DEFINED MOBILITY MANAGEMENT AND BASE STATION CONTROL FOR GREEN CELLULAR NETWORKS

Sunae Shin, Candidate for the Doctor of Philosophy Degree

University of Missouri–Kansas City, 2015

ABSTRACT

Mobile communication systems have revolutionized in order to fulfill exponentially increasing data traffic volume due to the introduction of new devices such as smartphones and tablets and success of social networking services. Evolving cellular networks include emerging technologies such as Software-Defined Network (SDN) and Network Function Virtualization (NFV). SDN is an emerging network architecture that allows dynamic and flexible network operations with centralized controller. NFV addresses the problem of a large and increasing number of hardware appliances and focuses on optimizing the network services themselves. With SDN and NFV, cellular networks are able to provide more flexible and agile management that can better align and support the mobile users.

In this dissertation, we address location management and handover to reduce data traffic toward the core network and to reduce energy consumption. Location management

is a key control task in cellular network operations. We propose and develop an efficient group location management scheme as a virtualized network function for group cellular applications. The performance improvement is mainly achieved by the virtualized and separate group management architecture and an efficient dynamic group profiling algorithm. We conduct theoretical analyses of our scheme for signaling costs and performance gains under diverse traffic conditions. Furthermore, we carry out extensive evaluations using both real traces and synthetic human mobility data, and we validate the efficiency of the proposed scheme in both location updates and paging.

Moreover, in order to tackle the issues of mounting deployments and large energy consumption of base stations, it is integral to devise schemes to improve energy efficiency in cellular networks. We propose a virtualized network function of cell management on an SDN architecture. We develop a cell management algorithm on the architecture that can effectively control the sleep and awake modes of base stations and perform handover operations in a cellular network. It provides significant benefits over current cellular networks that suffer from inflexible management and complex control. Our extensive trace-driven evaluation results show that the proposed control architecture and the cell management algorithm achieve significant energy savings, and incur less control message exchanges, more cells in a sleep mode for longer durations, and less cell status changes than existing energy saving approaches for cellular networks.

APPROVAL PAGE

The faculty listed below, appointed by the Dean of the School of Graduate Studies, have examined a dissertation titled "Software-Defined Mobility Management and Base Station Control for Green Cellular Networks ," presented by Sunae Shin, candidate for the Doctor of Philosophy degree, and hereby certify that in their opinion it is worthy of acceptance.

Supervisory Committee

Baek-Young Choi, Ph.D., Committee Chair
Department of Computer Science Electrical Engineering

Cory Beard, Ph.D.
Department of Computer Science Electrical Engineering

Ghulam Chaudhry, Ph.D.
Department of Computer Science Electrical Engineering

Masud Chowdhury, Ph.D.
Department of Computer Science Electrical Engineering

Sejun Song, Ph.D.
Department of Computer Science Electrical Engineering

CONTENTS

## ILLUSTRATIONS

TABLES

# ACKNOWLEDGEMENTS

First of all, I would like to express my deepest gratitude to my advisors Dr. Baek-Young Choi and Dr. Sejun Song for all their excellent guidance, advice, patience, and providing me with an excellent atmosphere for doing research. Their great advice and guidance during my Ph.D. studies contributed to my growth in research skills of reading papers critically, discovering ideas, building up projects, and ultimately leading and managing projects throughout all phases of research.

I would like to thank all of my committee members, Dr. Cory Beard, Dr. Ghulam Chaudhry, and Dr. Masud Chowdhury for all their help and sincere advices when I approached them with questions. Their comments have helped to clarify and improve this work. I also would like to thank all the lab mates Daehee Kim, Kaustubh Dhondge, Xinjie Guan, and Helen Gebre-Amlak for their support and suggestions.

Moreover, I sincerely would like to thank my parents Daehyun Shin and Youngboon Song and my husband's parents Youngwoo Park and Kyungsook Jang. Also, my brother Wooshik Shin and brother-in-law Youngjoo Cho. They were always supporting me and encouraging me with their best wishes.

Lastly, but most importantly, I'm grateful to my husband Hyungbae Park and my two adorable daughters, Katie Park and Claire Park, have always been my happiness and driving force during my doctoral research. Their love has been and will always be my momentum to move forward.

# CHAPTER 1

# INTRODUCTION

Cellular network systems is evolving and provide attractive data and communication services to fulfill a number of requirements and challenges. The data traffic of cellular networks is significantly increasing with introduction of new devices such as smartphones and tablets. In addition, the success of social networking services and associated applications the data traffic volumes in the networks have exploded during the last few years. In Ericsson's report, the data traffic is grown 55 percent between 2014 and 2015. In addition, the total number of mobile subscription is now around 7.3 billion by adding 87 million new subscriptions. Note that actual number of subscribers is around 4.9 billion, since many have several subscriptions [30]. Additionally, the global number of base stations predicted to reach up to 4 million by the end of 2015 to cover increased data traffic. Therefore, the core network will face congestion due to the increased mobile traffic and the number of base stations as a solution [52].

With increased data traffic and number of subscription, energy efficiency of cellular networks has received remarkable attention recently. A current estimation indicates that the Information and Communication Technology (ICT) infrastructure causes 3$\%$ of the world wide electricity consumption and 2$\%$ of global $CO_2$ emissions [3].

In order to keep up with the traffic growth, the networks need to optimize the current resources and also add new devices/technologies. However, current networks contain complex and inflexible devices. Furthermore, mobile users expect a high quality and continuous improvement on services. To ensure quality of users' experience, cellular operators find promising concepts and evolving to make the networks more agile, efficient and flexible. This can be achieved through virtualized network functions in LTE (Long Term Evolution) systems [18, 34], and Network Function Virtualization (NFV) architectures are being proposed [11, 57]. NFV addresses the problems of a large and increasing number of hardware appliances for individual network functions. By virtualizing network functions to commercial off-the-shelf servers, it can reduce capital and operating expenditures. Additionally, using Software-Defined Network (SDN) principle, redesign of the Radio Access Network (RAN) and improvement of cellular core networks can be addressed to obtain network flexibility and manageability.

In this research, we study on location management scheme for group applications to reduce traffic load to the cellular core network. Location management is one of the main operation in cellular networks that keeps track of users' movement to deliver calls and data. For the group of users who uses the same application, it is possible to reduce the number of location update with clustering the users based on their geographic location. By reducing the number of location update, we can alleviate a well-known bottle neck problem on the traffic load to the core network. The group location management scheme is handled as a virtualized network function in cellular network and improves group application service. Moreover, another virtualized network function for energy efficient eNodeB control is discussed. By decoupling the functionality of power control of eNodeB, we observe significant improvement on energy consumption in a cellular network. Centralizing the algorithm of cell management, it also greatly simplifies control over the sleep and awake modes of eNodeB by enabling an agile handover operations.

## 1.1 Location Management in Cellular Networks

The types of services of cellular networks are also being expanded beyond regular one-to-one calls. As a major example, Push to Talk over Cellular (PoC) is a service option for a cellular phone network that allows subscribers to make a call to a group of users with a single button. PoC service works as a walkie-talkie with an unlimited range. The connections should be made instantly, with little delay, with all the users in a group. Currently, only limited versions of the services are available by a few providers [2, 4, 6] and only for small scale enterprise users. The Open Mobile Alliance [5] is defining PoC as part of the IP Multimedia Subsystem [81]. Group applications over cellular networks, such as group audio or video conferencing and stream media broadcasting to a group, are limited in scale at the moment but will be prevalent in the near future.

The core issue of practical and large scale group call services is the performance. Here,address an important performance issue for efficient group location management. Location management is an essential task in cellular mobile networks that keeps track of the movements of individual users and updates a location record in the Home Subscriber Server (HSS). Location management schemes include two types of basic operations, namely i) tracking area update - a report made from a Mobile Node (MN) to the Mobile Management Entity (MME) when an individual user moves from a Tracking Area

(TA) to another TA (Location Area or LA in 3G term); and ii) paging - a message made by the MME to all cells in a TA to find a callee.

Many location management schemes have been proposed for regular *one-to-one* calls. In this paper, we call these approaches Individual Location Management (ILM) schemes. Such examples include [8, 17, 58, 63, 78] in which there is an attempt to make the location update decision based on a user's temporal and spatial movement patterns. However, the ILM approaches pose a substantial overhead of location management when they are used for a large number of group members and thus, become infeasible for practical use.

On the other hand, there are several *cluster-based* location management schemes recommended as well, such as [19, 38, 45, 51] where multiple users' location updates can be aggregated when they are clustered within a region.[1] However, they are still inherently designed for *one-to-one* calls and can't be directly applied to *one-to-many* group applications. This is because, for true PoC services, we can't mandate that all the MNs of a group application should belong to a single location area and should exhibit the same mobility pattern all the time, even though some similarity of group members' mobility may be temporarily present. For instance, a part of the group users may be located in different cities. Therefore, a proper location management scheme for *group applications* is an imminent need, especially to handle many groups with a large number of members in a scalable manner.

[1]The authors typically used the word 'group-based' in those articles. However, we use the word 'cluster-based' to refer them, in order to distinguish from the 'group', a type of applications in this paper.

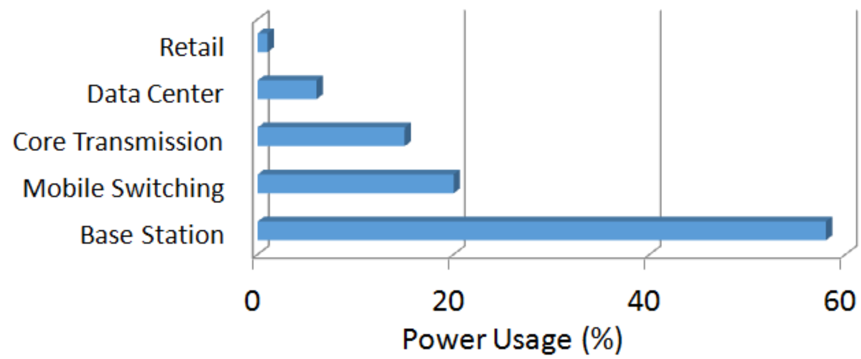


Figure 1: Power consumption of cellular network components

### 1.2 Green Cellular Networks

Energy efficiency of cellular networks has received remarkable attention recently with exponentially increasing deployments and rising concerns of the harmful effects to the environment caused by $CO_2$ emissions emitted from base stations. A current estimation indicates that the Information and Communication Technology (ICT) infrastructure causes 3% of the world wide electricity consumption and 2% of global $CO_2$ emissions. Moreover, it is observed that the power consumption of 16-20% per year corresponds to a doubling every 4 to 5 years [3]. Particularly, 60% of the total power consumption of the cellular networks is caused by base stations [37] as illustrated in Figure 1. It is predicted that the global number of base stations will reach up to 4 million by the end of 2015 [52].

Instigated by the alarm, several researches were conducted on minimizing base station energy consumption using improvements in power amplifiers or with load dependent power control. Most energy improvement proposals use the sleep mode of a base station based on energy-aware cooperation among neighboring base stations. Although, sleep mode can save energy consumption significantly, note that it may cause problems such as an activation time issue and a ping-pong effect [29]. Performance degradation is experienced during the activation time, and the ping-pong effect that is unnecessary for on/off oscillations can increase the energy consumption with frequent wake-up processes and handover control messages while decreasing the users' QoS. The problems intrinsically stem from the sleep mode decision that was made based on myopic information of immediate neighboring base stations. The radio access network of LTE or LTE-Advanced, E-UTRAN (evolved UMTS Terrestrial Radio Access), consists of eNodeBs that support flexible bandwidth deployments. The eNodeB is a complex base station (BS) that communicates with other eNodeBs and core network elements as well. eNodeBs are responsible for all radio related functions and handover decisions. However, there is no global, centralized control in the current E-UTRAN.

## 1.3 Software-Defined Cellular Networks

SDN is an emerging network architecture that allows dynamic and flexible network operations by decoupling the network control plane from the data plane [27]. The migration of control plan to the logically centralized controller simplifies the network management and enables new services.

Recently, there has been significant interest in integrating the SDN principles in current cellular architectures such as 3G Universal Mobile Telecommunications System (UMTS)and 4G LTE [66]. Current cellular network architecture has centralized data flow and all traffic passes through specialized equipment (e.g., Packet gateway in LTE). This leads to increase the management cost because of the complexity of the devices and raises scalability problems [52].

Introducing SDN concept to cellular network will provide a complete view of the whole network by decoupling the control from the data plane. This will allow network equipment to become simpler and reduce the overall infrastructural cost. Moreover, applying SDN to cellular networks can enable simple network management and give flexible design and operation on the cellular network. Redesign of the radio access network (RAN) using SDN principles for load balancing and utility optimization is proposed in [35]. Improvement of the scalability and flexibility of cellular core networks with SDN have been presented [43]. Meanwhile, the concept of NFV is proposed by a consortium of service providers [69] to address the problems of a large and increasing number of hardware appliances for individual network functions. By consolidating and virtualizing network functions to commercial off-the-shelf servers, it can reduce capital and operating expenditures.

Another study that gives the centralized control to RAN called cloud RAN (C-RAN) is presented in [55]. C-RAN centralizes the baseband processing resources into a pool to solve problems of network deployment, interference, and power consumption. The centralized control for RAN can support easy upgrade, multi-standard operation and maximum resource sharing. Additionally, C-RAN offers possibility for energy efficiency with reduced number of eNodeB sites and low transmission power. Although centralized control brings benefits to current cellular networks, both [41] and [36] pointed out the need of the virtualized architecture that virtualizes the base band unit (BBU) functionality and services in a centralized BBU pool.

## 1.4 Contribution of the Dissertation

In this dissertation, we focus on two aspects of cellular networks such as location management and energy saving on SDN and NFV architecture. the main contributions of this dissertation are as follows.

- We develop an efficient location management scheme for *group applications* in cellular networks. We propose a location management architecture that uses a so called Group Location Management (GLM) and dynamic group profiling of the members' geographic information. The group location management service can be augmented as a virtualized network function [69] either for a 3G or 4G cellular network architecture. The presence of GLM succinctly simplifies the group location management task and enables cellular network providers to handle a large number of members and groups. The group profiling algorithm dynamically updates its group members' location information with clusters of cells or location areas that can be of arbitrary shapes and sizes. We have validated the efficiency of the proposed scheme with theoretical analysis as well as extensive experiments. As for the experiments, we have used both real traces of human movements and synthetic human mobility data. Note that our scheme is complementary and beneficial to the traditional one-to-one call location management, but it is also interoperable with it.

- We propose an architecture of a virtualized network function of cell management on a software-defined cellular network, called Siesta (Software-defined energy efficient base station control) for green cellular networks. With the proposed architecture and network-wide information, we then employ a cell management algorithm that can effectively select a minimal set of eNodeBs that can serve all users without incurring a ping-pong effect. The ping pong effect is one of the well known problems in cellular networks that causes unnecessary frequent handovers. It increases control messages to the core network and decreases users' QoS. It also increases the energy consumption with frequent on-and-off status changes of eNodeBs. Siesta architecture reduces the communication overhead among cellular network elements. Siesta first reduces the control message between network elements due to the movement of the control plane from eNodeB to a Siesta NFV module. Furthermore, the message exchange necessary for the handover procedure is also decreased compared to the current LTE handover procedure. Through extensive evaluations using human mobility traces, we show that Siesta cell management scheme achieves substantial energy savings in a network over an existing state-of-the-art approach. We also demonstrate the stability of the eNodeB status from various perspectives. Additionally, we observed decrease number of eNodeB on and off and handover. Also, we observe the reduced energy consumption with longer sleep duration.

## 1.5 Organization

The rest of this dissertation is organized as follows. In Chapter 2, we give an overview on the issues of evolution of cellular networks, SDN, and NFV. Chapter 3 review related work dealing with the location management and energy saving with eNodeB cooperation. Also, the previous studies on cellular networks with SDN and NFV are discussed. In Chapters 4 and 5, we identify problems of cellular networks in regards to location management and energy efficiency and propose those as a virtualized network function. Finally, Chapter 6 summarizes and concludes this dissertation and discusses future research goals.

# CHAPTER 2

# BACKGROUND

Cellular network systems have revolutionized communication among people and provide services to make people connected over mobile networks. The First Generation (1G) refers to analog cellular technologies and has fulfilled the basic mobile voice. The Second Generation (2G) denoted initial digital systems and has introduced capacity and coverage. Currently, Third Generation (3G) and Fourth Generation (4G) technologies is evolving to fulfill challenges and expectations comes from significantly increased number of subscribers and a large amount of data over cellular networks [9].

Evolving cellular networks include emerging technologies such as SDN and NFV. SDN an emerging network architecture that allows dynamic and flexible network operations by decoupling the control plane from the data plane [27]. Introducing SDN to cellular networks can enable simple network management and give flexible design and operation on the cellular networks. Meanwhile, the concept of NFV is proposed by a consortium of service providers [69] to address the problems of a large and increasing number of hardware appliances for individual network functions. By consolidating and virtualizing network functions to commercial off-the-shelf servers, it can reduce capital and operating expenditures.

This chapter provides a high level overview of the evolution of cellular networks communication. In addition, we also include the objective and efficiency of SDN and

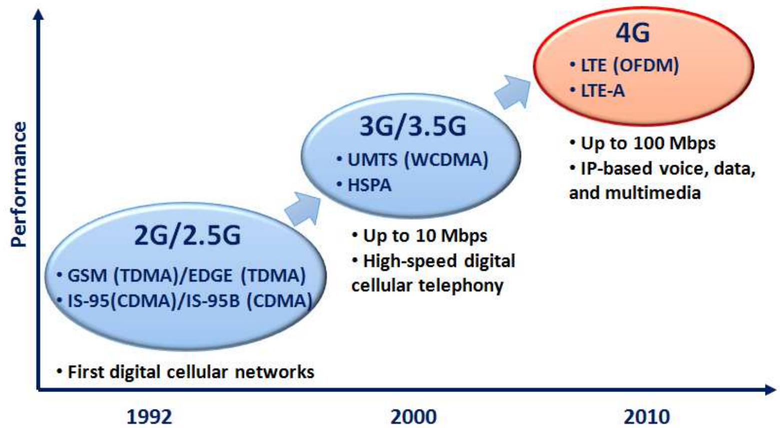


Figure 2: Evolution of digital cellular networks

NFV.

## 2.1 Evolution of Cellular Systems

In order to satisfy the requirements of data traffic and provide various services, cellular systems developed from the first generation to current LTE advanced networks. The 1G mobile system used analog transmission for voice services. Compared to 1G systems, 2G introduced digital multiple access technologies such as Time Division Multiple Access (TDMA) and Code Division Multiple Access (CDMA). The Global System for Mobile communications (GSM) was deployed in Europe that uses TDMA to support multiple users and provide standard. The main components of GSM system are Base Station Subsystem (BSS) that contains Base Transceiver Station (BTS) and Base Station Controllers (BSC). Also, the system includes Mobile Switching Center (MSC), Visitor Location Register (VLR), and Home Location Register (HLR) for mobility management

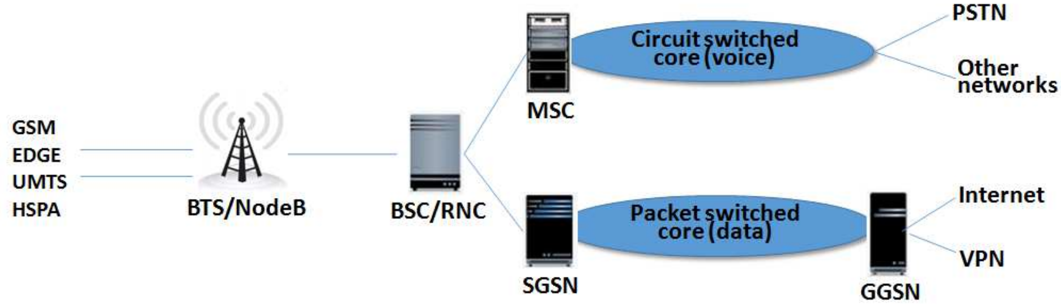


Figure 3: 2G/3G cellular network architecture [10]

of users. As data transfer increased, elements such as Servicing GPRS (SGSN) and Gateway GPRS (GGSN) were added. These elements handled the packet data and called Packet Switched (PS) core network. In the United States, IS-95 that uses CDMA was deployed.

The 3G was introduced since the need of providing services independent of the technology platform and whose network design standards are same globally. The International Telecommunication Union (ITU) defined the demands for 3G networks with the IMT-2000 standard and an organization called 3G partnership Project (3GPP) has continued the work by defining a mobile system. In Europe the system was called UMTS and WCDMA was used. The main elements were Base Station (BS, or NodeB), Radio Network Controller (RNC), and SGSN/GGSN. 3G includes wide-area wireless voice telephony and video calls in a mobile environment. Additionally, High Speed Packet Access (HSPA) data transmission which able to speed up to 14.4 Mbps on the downlink and 5.8 Mbps on the uplink. The summary of evolution of digital cellular networks is presented in Figure 2 and the architecture of 2G and 3G are shown in Figure 3 [10].

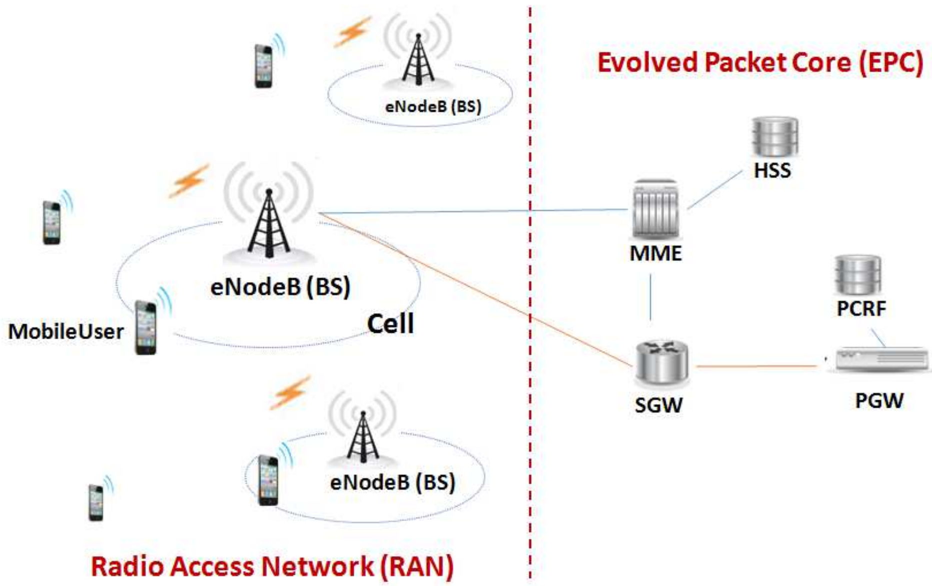


Figure 4: 4G (LTE) cellular network architecture

With exponentially increasing user demand and various services, industries provide 4G, all-IP, mobile communication systems. The main difference between 3G and 4G is that the functionality of RNC and BSC is now distributed to the eNodeB (evolved NodeB) and gateways. Evolved Packet Core (EPC) is a new, all-IP based mobile core network for the 4G networks. The EPC provides functionalities that 2G/3G has achieved through two separate domains: CS for voice and PS for data [10]. Current LTE cellular architecture of 4G is shown in Figure 4. In LTE networks, a logical group of cells is called the Tracking Area (TA) and the ID of the TA is broadcast by its eNodeB (similar to the Base Station in 3G networks). The TA information of an mobile user is tracked by the MME. The MME is the control node that processes the signaling between the mobile user and the core network. The location information of the mobile users resides to the HSS(similar to the HLR in 3G networks). The mobile users can be in two modes: 'idle' and ’connected.’ The idle mode means that the mobile user does not have a dedicated connection to the network, but the mobile user listens to the broadcast channel. A connected mode means that a mobile user has a dedicated connection to the network and has voice or data transmission.

Although current cellular networks are providing high quality services for their subscribers, it is challenging to satisfy all the requirements. The limitations of current networks are listed as below [52].

- Complex network management: Most of the backhaul devices has lack of common control interfaces. Configuration and policy enforcement requires a proper amount of effort.

- Inflexibility: Due to the manually intensive service activation and delivery, implementation of new service takes weeks or months. Also, introducing new services takes several months or years since the standardization process is a long lasting process.

- Complex and expensive network devices: The devices in the core network such as Packet data network Gateway (PGW) are responsible for many significant data plane functions.

- Higher cost: The operators do not have flexibility to handle the devices from different vendors. This increases the Capital expenditure (CAPEX) and the manual configuration increases the Operational expenditure (OPEX).

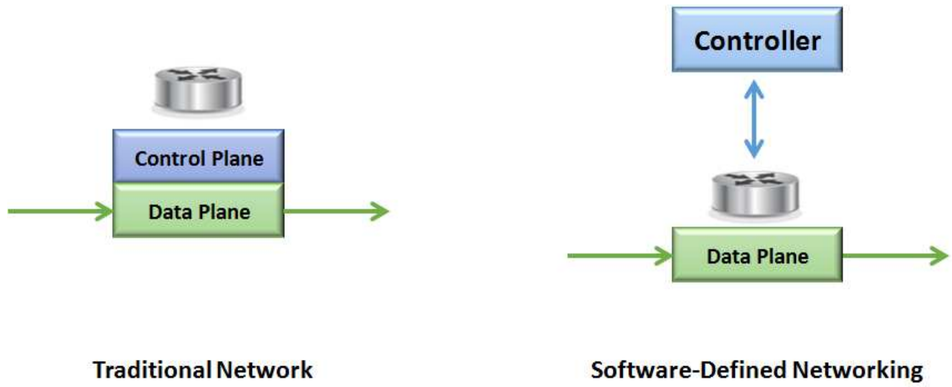

Figure 5: Comparison of traditional network and software-defined networking

### 2.2 Software-Defined Networking

SDN is an emerging network architecture that supports programmable interface which provides flexibility and agility on the network control management. The SDN architecture allows dynamic and flexible network operations by decoupling the network control plane from the data plane [27]. Decoupled control plane is abstracted to interact and handle all the underlying network devices and called SDN controller. The SDN controller can run on a commodity server and gives logically centralized control. This migration of control simplifies the network management and enables new services. SDN is originally designed for fixed networks, but it also gives the benefits to wireless networks that have different requirements such as mobility management, efficient protection of the air interface, and higher quality of service.

Here, we present the various benefits of adaption of SDN concepts wireless networks [52].

- Logically centralized controlling: A centralized control make decision for control plane based on the global view of the network. Compare to the existing mechanisms, the decisions are more accurate, optimum and efficient.

- Flexibility: The controller is able to control any SDN-enabled network component from any vendor. This allows network operator to mix and match the network elements from different vendors.

- Higher rate of innovation and opportunity for new services: The network programmability and common Application Programming Interfaces (APIs) accelerates business innovation in the networks. The operators are allowed to test various novel applications for quick innovation.

- More granular network control: Dynamic change on control policies based on the network behaviors is possible because the flow control policies are applied at a very granular level.

- Heterogeneous network support: End-to-end communications across heterogeneous network technologies such as GSM, 3G, and 4G can be provided with flow-based traffic transport model.

Introducing SDN to cellular networks enables simple network management and give flexible design and operation on the cellular network with the benefits above. The decoupled control plane is illustrated in Figure 5 and compared with traditional network.By

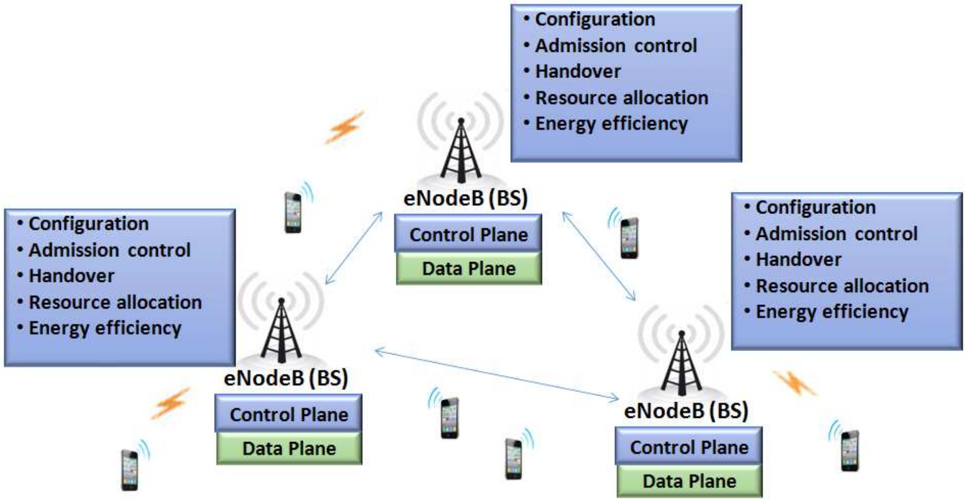


Figure 6: Control plane and data plane in current cellular networks

applying SDN to cellular network, we bring the benefits of SDN to current cellular networks. As presented in Figure 6, both control plane and data plane resides on each eNodeB in current cellular networks. Thus, all the control plane management such as admission control, handover, and resource allocation is controled by each eNodeB. Also, a set of eNodeBs is involved in order to make decision on network management. Compare to current networks, Figure 7 illustrates that control plane of each eNodeB is moved to SDN controller. With migration of control, eNodeB control and network management is simplified. Furthermore, the controller has centralized view of the network and brings many benefits such as reduced management cost and agility on new service deployment.

Recently, a number of studies from universities and industries have been involved to develop and improve cellular network with SDN architecture. Redesign of the RAN using SDN principles for load balancing and utility optimization is proposed in [35]. Improvement of the scalability and flexibility of cellular core networks with SDN have

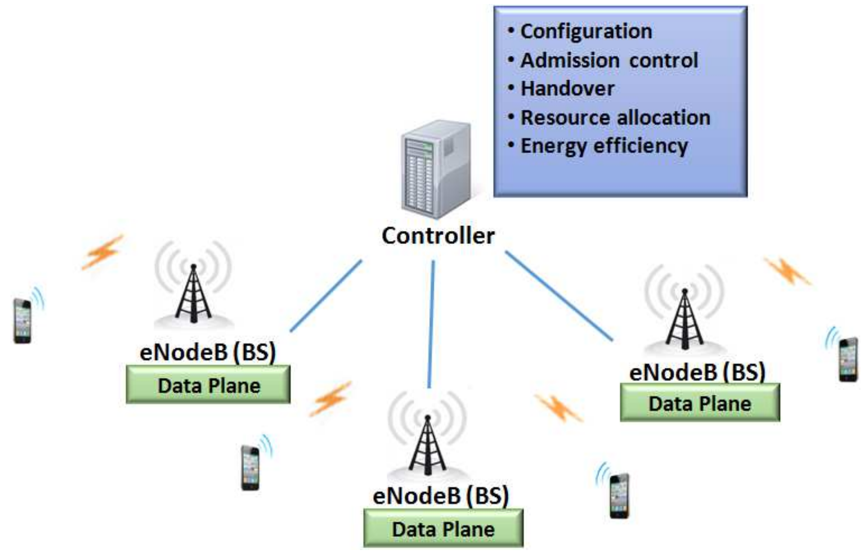


Figure 7: Control plane and data plane in cellular networks with SDN

been presented [43].

### 2.3 Network Function Virtualization

Meanwhile, the concept of NFV is proposed by a consortium of service providers [69] to address the problems of a large and increasing number of hardware appliances for individual network functions. NFV aims to leverage standard IT virtualization technology to consolidate many network equipment types onto industry standard high-volume servers, switches, and storage [32]. By consolidating and virtualizing network functions to commercial off-the-shelf servers, it can reduce capital and operating expenditures. The control functions in eNodeB that can be virtualized are showned in Figure 8.

Although NFV can be implemented without a SDN being required, the two approaches can be combined and has potential of greater results. While NFV concentrates

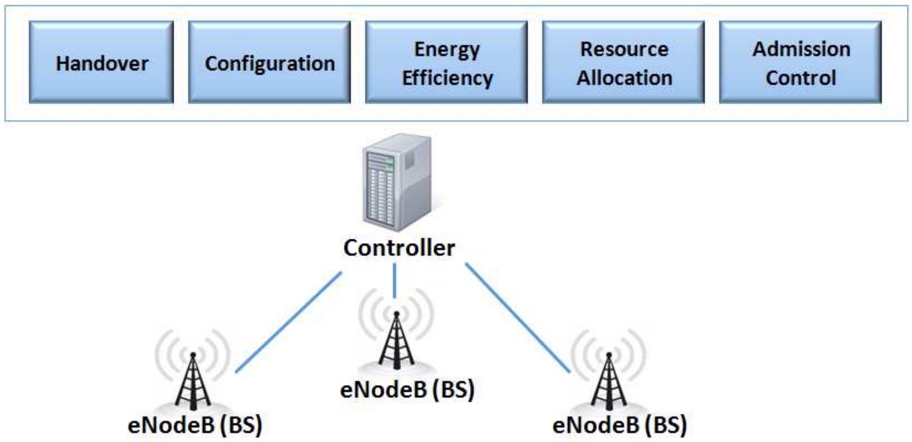


Figure 8: Cellular networks with virtualized network function

on the services, SDN focuses on the network automation that enables policy-based decisions to orchestrate which network traffic goes where. These two technologies are the key to innovate the network to keep pace with the requirements of mobile users and devices its connecting [32, 69].

# CHAPTER 3

# RELATED WORK

Before we discuss our proposed methods, this chapter presents previous works on individual location management and cluster-based location management. Additionally, we discuss BS sleep/wakeup schemes and evolving cellular network with SDN and NFV. Based on the previous works, we point out the problems and insufficient part for the future cellular networks.

## 3.1 Related Work of Location Management in Cellular Networks

Location management is necessary in cellular networks in order to keep track of idle mobile users within the network and forward calls. There are two main tasks in location management, namely the tracking area update and paging. A tracking area update is an operation by which a mobile user reports its new location, and paging is initiated by an eNodeB when an incoming call arrives to find the callee's location. Once a mobile user moves to a new TA, a mobile user needs to perform a tracking area update to keep its location updated in the MME. When the network needs to forward an incoming call or data to an idle mode mobile user, the MME sends a paging message to all cells in the mobile users' last registered TA.

A TA is a group of cells that may be static or dynamic. The number of cells in a TA impacts the signaling traffic of the tracking area updates and paging. The higher computation and separate data storage for each mobile can be caused by dynamic TAs. However, it can adapt to the mobility and call pattern of the mobile users resulting in reduced signaling traffic. The static TA has been used in most of the current location management systems, such as GSM, UMTS, and CDMA2000. In LTE, a mobile node maintains a list of tracking areas that geographically center around the initial location [50]. Since it is still only for one-to-one calls, it is not readily made efficient for group communications as it is. On the other hand, LTE provides a flexible architecture for virtualized network functions.

Many location management schemes have been proposed for regular one-to-one calls (thus, using an individual based approach) such as [8, 17, 58, 63, 78] that attempt to make the tracking area update decision based on a user's temporal and spatial movement patterns. Defining a TA or LA has been studied extensively to improve the performance of location management. In [22], a method for selecting the optimal set of cells for each static TA is proposed. Compared to a static TA, techniques for a dynamic TA are proposed to dynamically adjust the size and shape of the TA for each individual MN. The TA varies based on the MNs' movement patterns and reduces the location management signaling traffic overhead. The improved performance of dynamically overlapped TAs is shown in [24, 76, 77].

A few techniques using algorithms of the neural network are suggested to add intelligence in location management systems. In [71], a profile-based scheme is improved to reduce the location update cost by combining back-propagation algorithms that implement the learning process. The location prediction methods are proposed in [61] based on the users' movement history and the current state of the user.

Although these approaches would provide improved location management for one-to-one calls, they do not exploit the redundancy of the mobility pattern that may exist in group call applications. Furthermore, they do not address the significant burden on a server and the control traffic overhead in the HLR or HSS for group calls that lead to performance degradation.

*Cluster-based* location management schemes have been proposed in [19, 38, 45, 51]. There are several extra-steps necessary for such cluster-based management approaches, including cluster establishment, cluster maintenance, and cluster leader selection. Since only the cluster leader performs a location update on behalf of other cluster members, this reduces the cost of tracking area updates. Note that cluster-based location management approaches can only apply to a cluster of users who share a similar mobility pattern and cannot be directly used for location management for group applications. The mobility pattern of the mobile nodes may not be the same (nor similar) for all mobile nodes belonging to a group application.

Despite its crucial need, there has been little work to address the issue of *group applications* in cellular networks. To the best of our knowledge, our work is the first to study location management for group applications that aims to reduce the costs of both tracking area updates and paging. We introduce the concept of a GLM that employs group

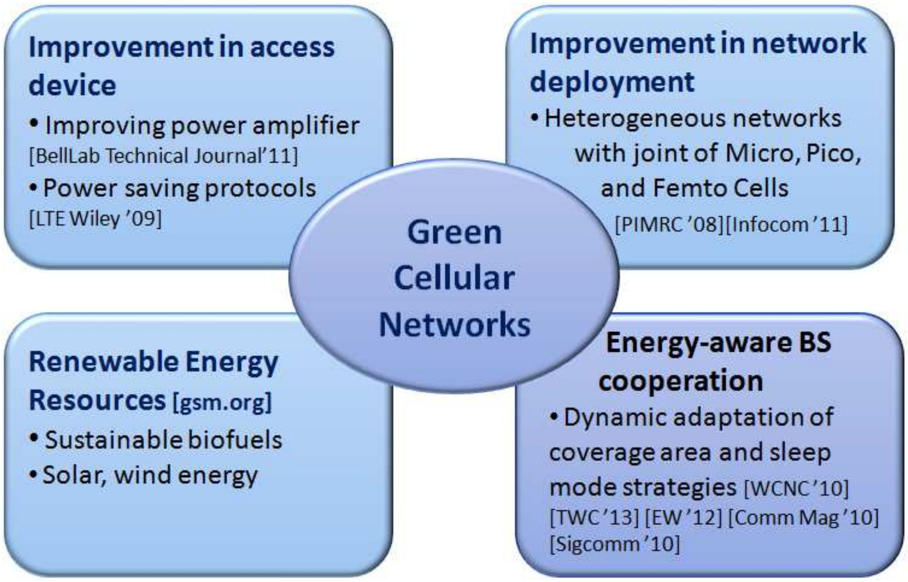


Figure 9: Studies on energy saving in cellular networks

profile-based location management. GLM architecture is different from group-based profiling architecture, as it is capable of handling profiles of a large group distributed in a large area, whereas a group-based scheme can only deal with a profile within one TA.

### 3.2 Related Work of eNodeB Cooperation for Energy Saving

The concern on large energy consumption in cellular networks has triggered many research efforts to reduce eNodeB energy usage. The control of power in eNodeB is one of the main methods for energy saving. Limiting power transmission that can reduce both the amount of interference and energy consumption is discussed in [44]. However, it is challenging because decreasing the eNodeB transmission power implies a limited impact on the quality of service. In [72], dynamic power control during a period of low load such as nighttime is suggested while ensuring full coverage at all times.

Another dominant energy saving technique for eNodeB is energy-aware cooperation in eNodeBs. Significant fluctuations of traffic load in cellular networks in space and time due to users' behavior is considered for eNodeB cooperation. Limited cell size adjustment called "cell-breathing" is suggested in [20]. The mobile user is handed off to the neighboring cells by reducing a cell size through power control if the cell is under heavy load or interference. Similarly, a more flexible concept called "Cell zooming" is presented in [59]. Cells adjust their size according to the network or traffic situation in order to balance traffic load and reduce the energy consumption as well. Cell zooming also allows the eNodeB sleep mode for energy saving, while the neighboring cells can zoom out and help serve the mobile users cooperatively. For the cell zooming process, both centralized and distributed algorithms have been developed. More on the eNodeB sleep mode that is based on traffic load is presented in [40, 56, 67]. The traffic forecasting technique for the sleep mode control is based on the daily traffic that was studied in [70]. The quality of service (QoS), which is a significant issue in cellular networks, has been considered with control of the eNodeB sleep mode. In [29], the eNodeB activation and deactivation policy maximizes multiple object functions of the QoS and energy consumption, and in [21] each eNodeB estimates the distance of its mobile users and switches off if there is no degradation of the QoS.

Moreover, concept of Self-Organizing Networks (SON) have been introduced in 3GPP standard that enables network management such as optimization and reconfiguration to heal itself in order to reduce costs and improve network performance and flexibility [13]. The concept of SON can be applied to achieve a large number of objectives.

In [68], different use case for SON are discusses such as load balancing, cell outage management, and management of relays and repeaters. The power efficiency and the performance of SON techniques are investigated in [53, 54].

Recently, heterogeneous network deployment based on smaller cells such as micro, pico, and femto cells has emerged as a promising technique that can possibly reduce the energy consumption in cellular networks. In [26], the simulation shows that joint deployment of macro and pico cells can reduce the total energy consumption by up to 60% compared to a network with macro cells only. Additionally, micro eNodeB deployment and switching on-and-off schemes of macro and micro eNodeBs are presented in [73].

Most previous studies are based on the predictable traffic variation in space and time such as higher traffic during the daytime and a lower traffic situation at nighttime [40, 56, 67, 70]. Our work is unique in that we exploit information beyond immediate neighboring cells which is a global view of the network for better decision on energy saving. To the best of our knowledge, our work is the first to propose an NFV for a cellular network operation. Using SDN architecture, we could employ a cell management algorithm that yields the best energy efficiency as well as cell stability.

### 3.3 Related Work of Cellular Networks with SDN and NFV

Current cellular networks supports a number of subscribers who has frequent mobility and realtime control and services. In addition, various types of services and larger amount of data over cellular network presents challenges in cellular networks. These features bring emerging network architecture, SDN and NFV, to evolving cellular network to achieve challenges [12, 48].

SDN allows migration of control-related functions to SDN controller and simplifies the network management. Redesign of the RAN using SDN principles for load balancing and utility optimization is proposed in [35]. Improvement of the scalability and flexibility of cellular core networks with SDN have been presented [43]. NFV is known as complementary approach to SDN that focuses on optimizing the network services. The architecture of virtualized evolved packet core (vEPC) that takes full advantage of NFV and SDN is presented in [12]. vEPC provides flexibility in network configuration and management and also accelerates the delivery of new services. Additionally, the concept of virtualized radio access network (vRAN) that supports centralized radio base station is introduced in [36]. In thier vRAN architecture, multi-site/multi-standard baseband unit (MSS-BBU) is introduced for the flexible future cloud-based RAN structure. The architecture includes multiple remote radio heads (RRHs) and one set of MSS-BBUs and a cluster of RRHs represent a new multi-standard cloud base station. Integration of SDN and NFV on RAN is suggested in [28]. They pointed out the proposed architecture provies benefits such as efficient operation, lower power consumption, agile traffic management and high reliability.

Centralized control to RAN by decoupling BBU and RRH called cloud RAN (C-RAN) is also presented in [55]. C-RAN centralizes the baseband processing resources into a pool to solve problems of network deployment, interference, and power consumption. The centralized control for RAN can support easy upgrade, multi-standard operation and maximum resource sharing. Additionally, C-RAN offers possibility for energy efficiency with reduced number of eNodeB sites and low transmission power.

# CHAPTER 4

# DYNAMIC LOCATION MANAGEMENT SERVICE

In this chapter, we describe the proposed group location management scheme. We first introduce the concept and role of the virtualized network function for group location management (GLM). GLM manages the information of the group, group members, and the corresponding tracking areas with cluster profiles. Then, we discuss a dynamic profile-based TA generation algorithm. Finally, we demonstrate how the location management scheme works with the GLM and the dynamic profiles.

## 4.1 Virtualized Network Function for Group Location Management

In order to accelerate the performance of group applications and alleviate signaling traffic to/from the MME, we introduce a virtualized network function for group applications as described in Figure 10. GLM is one of the virtualized network functions (VNFs) that supports group applications.

Group members are the users of the same group applications and therefore, a message to a group should be sent to all the members. They are likely, but not necessarily, to share common activity areas and mobility patterns. Furthermore, each group is periodically profiled into clusters according to their geographic similarity by our dynamic profiling algorithm to economize location management costs. Note that the meaning of 'groups' used here is different from the one used in [19, 38, 45, 51], where groups indicate


Figure 10: Virtualized network function for group location management

a set of nodes that do share the same location area and mobility pattern, irrelevent to group application call types.

A typical record for a group in GLM contains the description of the group, group members, and the corresponding location areas with cluster profiles that are explained later. The used notations pertaining to the GLM are summarized in Table 1. Assume $K^g$ is the set of users belonging to group $g$, where $|K^g|$ is the number of members in this group, and $m^g(\in K^g)$ is an MN Id in the group. When a group member roams out of its current TA, $L_i^g$, that consists of adjacent cells $c_i^g$, the tracking area update will be performed by a group member to the GLM. Here, $i$ indicates the cluster ID $i^g$ of group $g$. Note that the tracking area update and updated information are handled by the GLM without involving the MME.

When an incoming group call arrives, a paging request will be sent to the MME from the GLM. The GLM will send the TA information of the group with a paging request. With the TA information of the group, the MME doesn't need to lookup the group members' tracking area stored in the HSS individually. The detailed processes of location update and paging for group location management are demonstrated in Section 4.3.

Table 1: Explanation of notations for group location management

| Notation | Explanation |
|---|---|
| $g$ | Group Id |
| $K^{\mathbf{g}}$ | Set of group users belonging to group $g$ |
| $m^{\mathbf{g}}$ | MN Id before group profiling, $m \in K$ |
| $i^g$ | Cluster Id of group $g$ |
| $m_i^g$ | Member Id of cluster $i$ of group $g$ |
| $\mathbb{P}_i^g$ | Profile of cluster $i$ of group $g$ |
| $L_i^g$ | Index for tracking area for cluster $i$ of group $g$ |
| $A^{\mathbf{g}}$ | Set of cells visited by group g |
| $c$ | Cell Id |
| $c_i^g$ | Cell Id in location area $L_i^g$ of group $g$ |
| $\check{p}$ | Residency probability matrix, size of which is $(\vert K\vert + 1) \times \vert A\vert$ |
| $\check{p}[m, c]$ | Probability that MN $m$ stay in cell $c$, where $m \in K$ |
| $\check{p}[\vert K\vert + 1, c]$ | Summation of probabilities of group members stay in cell $c$ |
| $p$ | Popularity array |

### 4.2 Dynamic Profiling Algorithm

We propose dynamic profiling algorithm based on Density-Based Spatial Clustering of Applications with Noise (DBSCAN) [31]. Dynamic profiling algorithm composed with combination of density-based clustering algorithm and grid-based clustering algorithm. DBSCAN is based on local connectivity and density functions. It discovers clusters of arbitrary shape and handle noise. Additionally, only one scan is needed to discover clusters. Although DBSCAN generate clusters for static objects, our improved algorithm considers mobility by using cell residency probability and profile. Cells which are in the

Table 2: Comparison of clustering algorithms

| Density-based clustering algorithm (DBSCAN) | Grid-based clustering algorithm (STING) | Profile-based cluster algorithm (dynamic profiling algorithm) |
|---|---|---|
| One scan | Once for each grid | One scan |
| Arbitrary shape and size | Arbitrary shape and size | Arbitrary shape and size |
| Handle noise | Not sensitive to noise | Consider noise as a group |
| No consideration on mobility | No consideration on mobility | Consider mobility |
| Maximum radius of the neighborhood and Minimum number of points of that point | count, mean, s, min, max, and type of distribution (normal, uniform, etc.) | Cell-based residency probability, weight on profile, and threshold |

same LA should be adjacent and minimum number of group members is 1. Furthermore, we periodically regenerate cluster for mobile users. Table 2 shows comparison of existing clustering algorithms with our suggested algorithm dynamic profiling algorithm. A conspicuous point of dynamic profiling algorithm is consideration of mobility on users. In addition, dynamic profiling algorithm can detect a group which has only one member since noise is also considered as a separate group.

To build clusters, we use member's movement pattern such as cell residency probability. Aggregated cells based on the cell residency probability create cluster. The area which contains members of the same cluster is considered as a one TA. Cell residency probability is used as an input of dynamic profiling algorithm. In previous group management schemes, assumption is presented that group is initially defined. In our case, however, group is not defined. Group members do not know each other or number of members. In addition, the range and the shape of clusters are variable. Members have

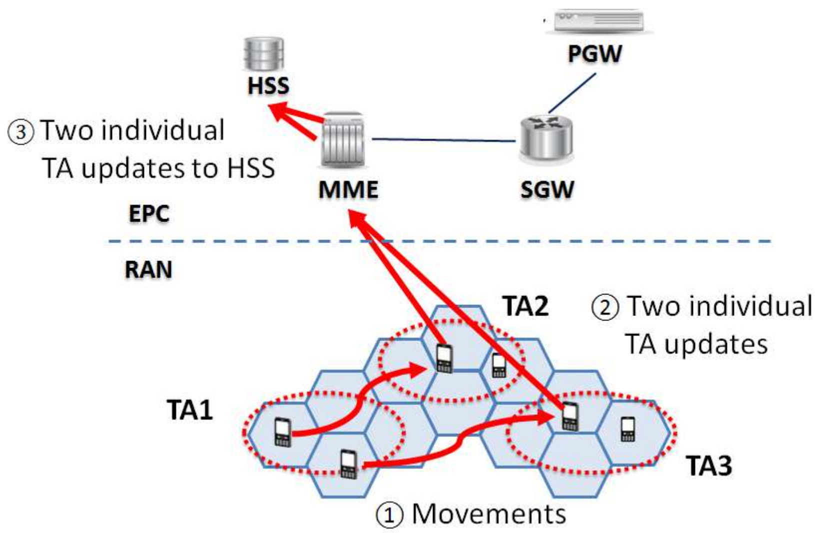


Figure 11: ILM location update procedure

regular mobility pattern. However, group does not have mobility pattern. Thus, cluster mobility pattern is random. We periodically regenerate cluster as designated in dynamic profiling algorithm. Furthermore, we put more weight on previous profile. This gives smooth change on the profile.

We now present our dynamic profiling algorithm that clusters adjacent areas into arbitrarily shaped and sized TAs according to the MNs' resident popularity in those areas. We develop the dynamic profiling algorithm by enhancing the DBSCAN that is designed for static objects, while cellular network users keep roaming without pre-determined mobility areas. Also note that the entire coverage area is naturally partitioned into cells managed by the deployed base stations. Therefore, we can consider the density on each cell area rather than the density of each subscriber's neighborhood as considered in the DBSCAN. This allows us a significantly lower computational time than in the DBSCAN.

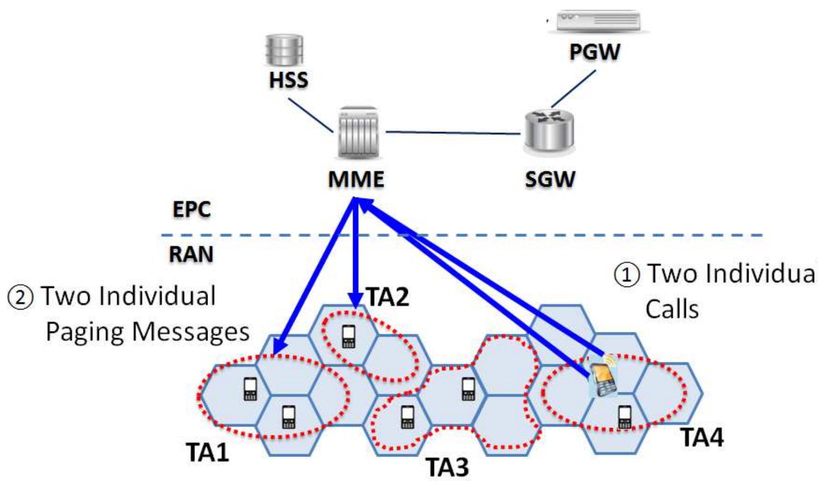


Figure 12: ILM paging procedure

In our dynamic profiling algorithm, historical mobility, a weight ($\alpha$), and a threshold ($\theta$), are used for profiling proper clusters that consist of a number of adjacent cell areas. As presented in Algorithm 1, the dynamic profiling algorithm starts with an arbitrary cell $c$ that has not been visited, and the current popularity $p[c]$ of cell $c$ will be calculated with the popularity in the last moment $p'[c]$. The computation of the average residency probability $p[c]$ is

$$p[c] = \alpha \cdot p'[c] + (1 - \alpha) \cdot \check{p}[|K| + 1, c] \tag{4.1}$$

where $\check{p}[|K| + 1, c]$ is estimated from the residency time of the group users in this cell area, and weight $\alpha$ is employed to balance the influence of historical popularity $p'[c]$ and current popularity $\check{p}[|K| + 1, c]$. For the sake of smoothing the TA changes, we suggest putting more weight on the previous popularity.

After that, $p[c]$ is compared with threshold $\theta$, and if it is larger than $\theta$, a cluster $i^g$

is formed and all users roaming in this TA belong to $i^g$. Furthermore, adjacent neighbors are queried. If spatial adjacent clusters exist, they will be combined to reduce tracking area update costs.

The dynamic profiling algorithm requires a little computational time and memory space. It costs $O(|K^g|)$ time to browse the residency probability for each user, where $|K^g|$ is the number of users in group $g$, then $O(|A^g|)$ time for traveling every cell area to cluster the entire coverage area, where $|A^g|$ is the number of cell areas visited by group $g$. Finally, it takes $O(1)$ time to all the neighbors of each cell area, and it maintains a matrix to record all neighbors for each cell in advance. Consequently, the total time complexity of the dynamic profiling algorithm is $O(max\{|K^g|, |A^g|\})$, where $|K^g|$ is the number of group members in $g$ and $|A^g|$ is the number of cell areas visited by $g$. Compared to the time complexity of the DBSCAN, which is $O(|A^g|log|A^g|)$ using an $R^*$ tree or $O(|A^g|^2)$ without indexing [31], our algorithm has a smaller time complexity.

On the other hand, the dynamic profiling algorithm occupies $\Theta(|A^g|)$ space for the neighborhood for each cell area and $\Theta(|K^g|)$ space to track each subscriber's residency probability. Therefore, the total space complexity of the proposed dynamic profiling algorithm is $\Theta(max\{|K^g|, |A^g|\})$.

### 4.3 Group Location Management Procedure

With the assistance of GLM and the dynamic profiling algorithm, the group location management can efficiently perform cellular localization with minor changes in current cellular networks. The location management of one-to-one calls may not be changed

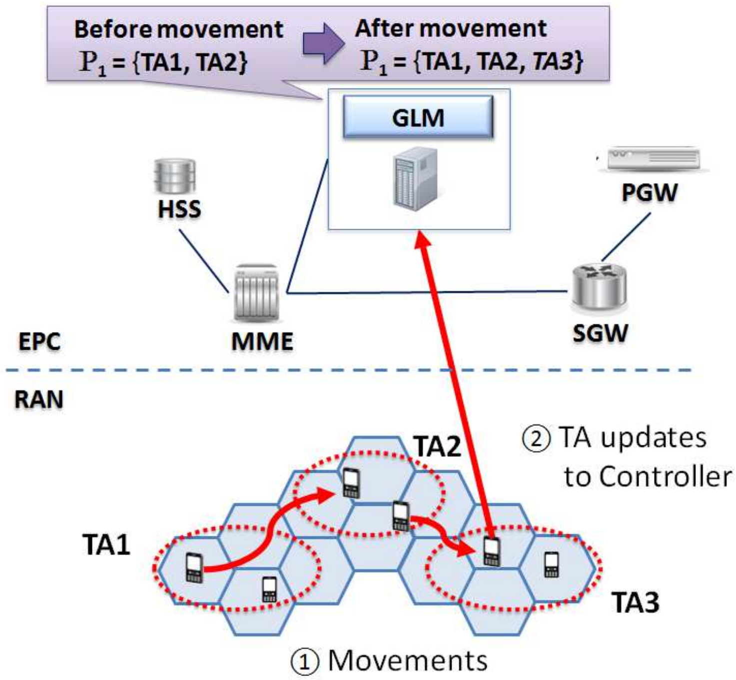


Figure 13: Proposed tracking area update with GLM

with this GLM scheme. However, GLM can be of assistance in the MME's maintaining the updated location information in an efficient manner using aggregated information.

Our proposed group location management scheme includes three algorithms: a profiling algorithm, a tracking area update algorithm, and a paging algorithm. A profiling algorithm is proceeded by GLM in order to partition a profiled area into non-overlapping groups of cells that are TAs. This process is presented in Algorithm 1 and arbitrary shaped and sized TAs are depicted in Figure 13. After the group profiling, TAs can be enlarged or shrunk by the MNs' movement and shape can be changed as well. The GLM also assigns a unique Id for each TA and the TA Id, and profiles of the group are periodically broadcast from the BS to the MNs as described in Algorithm 2.

The procedure of the group location management tracking area update is shown

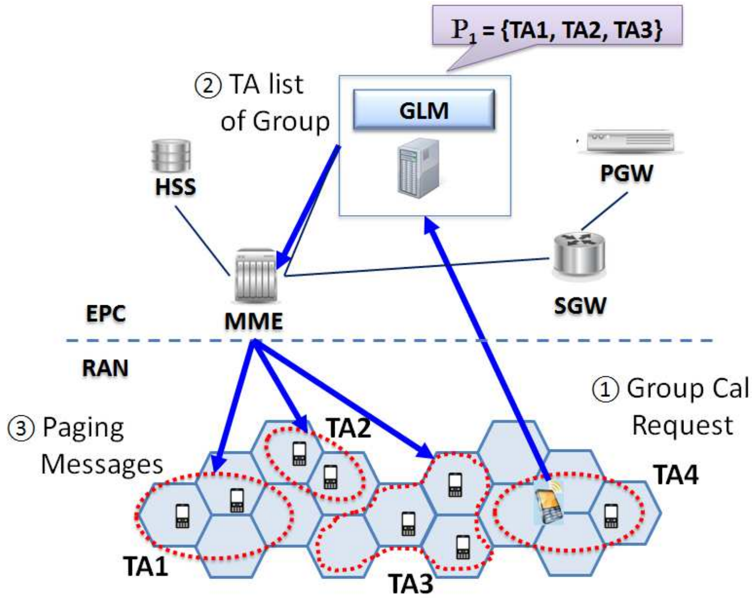


Figure 14: Proposed paging with GLM

in Algorithm 3. Compared to the tracking area update of the ILM, the GLM shows a less number of tracking area updates. In Figure 11, there are two different tracking area updates, since there are two different MNs' TA boundary crossings. However, not all the TA boundary crossings generate location updates in GLM tracking area update. In Figure 13, there are two different movements, an MN $m_1^1$, which is across the boundary from $L_1$ to $L_2$ and $m_2^1$, which is across the boundary from $L_2$ to $L_3$. Whenever the MNs sense a TA change, the MNs check whether a new TA Id is in the profile of the group or not. In this example, only one tracking area update from $m_2^1$ is performed since the new TA Id of $m_1^1$, $TA_2$, is already in the profile of group Id 1. Then the tracking area update message for $TA_3$ is sent to the GLM. The GLM responds with a confirmation message to the MN who just moved into $L_3$.

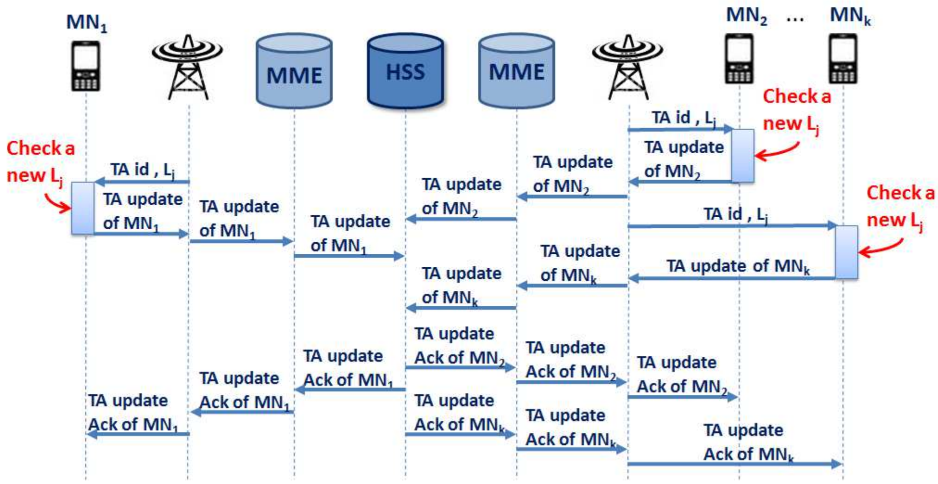


Figure 15: Sequence diagram for ILM tracking area update

Additionally, the number of paging messages is also reduced with the group location management scheme. As described in Figure 12, ILM's paging requires two individual paging messages in order to send two different calls even though the callees are in the same TA, while we observe that GLM sends a paging message once for all the group members in Figure 14. In the figure, a group call is initiated to members of group 1, the call travels through the GLM and paging area determined by the group profile of group 1. The GLM simplifies the paging process and reduces the traffic to the MME. Furthermore, the size of the paging area and delay can be reduced by simultaneously paging the last updated TA for each cluster. The procedure of this paging scheme is shown in Algorithm 4.

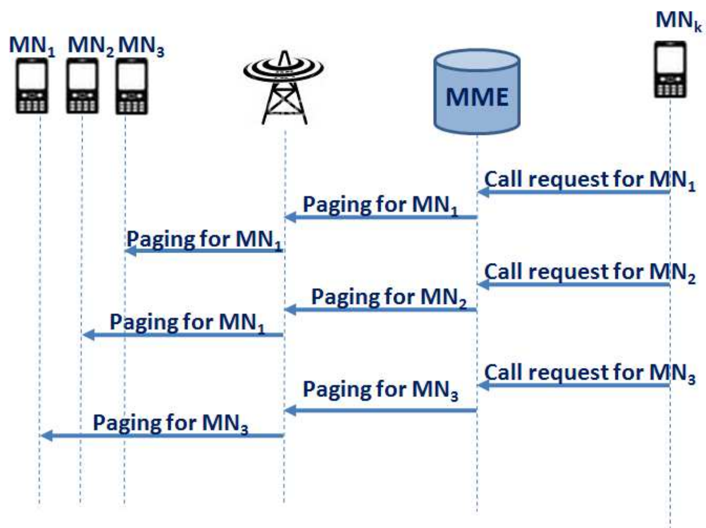


Figure 16: Sequence diagram for ILM paging

### 4.4 Benefits of Group Location Management

The benefits of our proposed group location management scheme are two fold. First, movements outside of a tracking area are reported to the GLM instead of the MME, which diminishes the overhead of control traffic to/from the MME and the database lookup operation [46, 64]. This alleviates the performance problem of the HLRs and VLRs in the GSM, UMTS, and CDMA2000 cellular networks [23], and MMEs in the LTE [50]. Second, the centralized information on the GLM makes it possible to perform dynamic profiling of a group rather than individuals, and this leads to fewer tracking area updates and paging costs, as analyzed in Section 4.5.

In order to elucidate how the interactions and order of processes are different between ILM and GLM, we describe both ILM and GLM with sequence diagrams. While ILM simply checks the new TA Id with the previous TA Id to make the decision for a

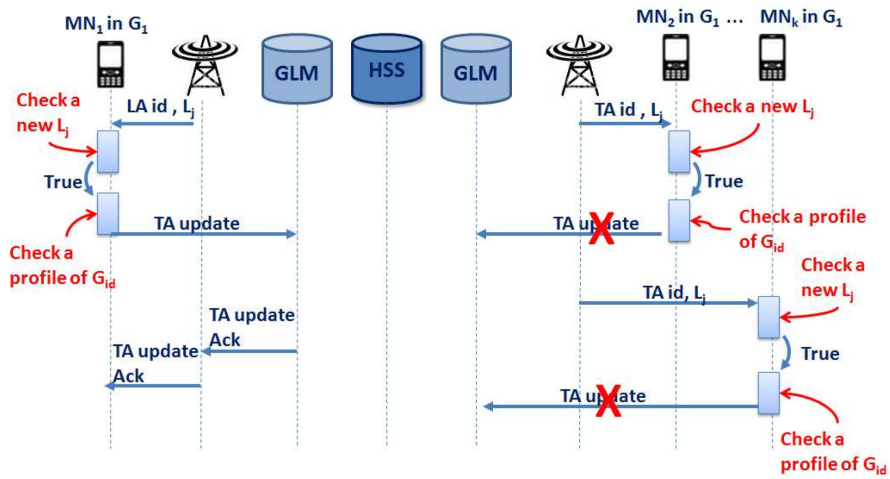


Figure 17: Sequence diagram for GLM tracking area update

tracking area update, GLM compares the new TA Id with the profile of the group in which the mobile user belongs. As shown in Figure 15, every mobile user needs to perform a tracking area update even though mobile users are in the same group; however, Figure 17 shows that GLM reduces the number of tracking area updates by confirming the group profile. Paging also takes benefits. Compared to the ILM in Figure 16 that sends a paging message to each mobile user, the GLM in Figure 18 sends a paging message only once for all the members of the group since the paging messages processed by the TA Id. The GLM enables this by checking the TA Id in periodically updated group profiles so that there can be reduced interaction to the MME.

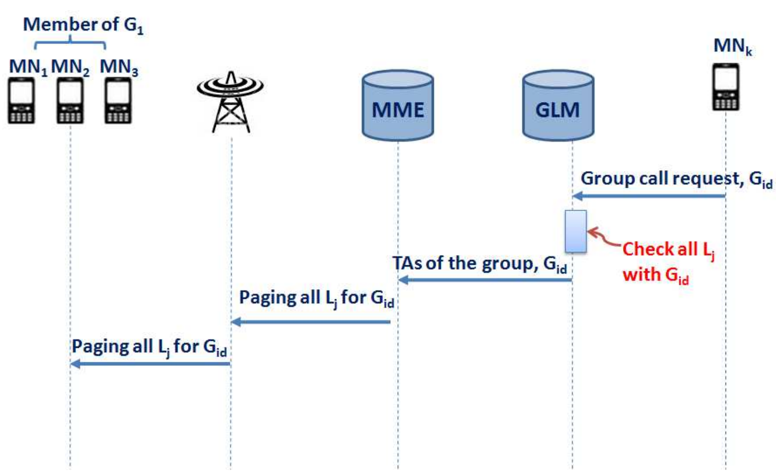


Figure 18: Sequence diagram for GLM paging

**Algorithm 1** Dynamic profiling algorithm

**input** Residency probability matrix $\check{p}$, popularity array $p$, $\alpha$, $threshold\ \theta$
**output** cell areas in each cluster; group user Ids in each cluster
**for** every user $m^g \in K^g$
    Cumulate $\check{p}[m, c]$ for cell area $c$ in $\check{p}[(|K| + 1), c]$;
**end for**
**for** each cell area $c$ that has not been visited
    mark $c$ as visited;
    calculate $p[c] = \alpha \times p[c] + (1 - \alpha) \times \check{p}[(|K| + 1), c]$;
    **if** $p[c] > \theta$
        construct a new cluster $i^g$;
        put all spacial adjacent cells in a new set named $Neighbor$
        **for** each cell area $b$ in $Neighbor$ and $p[b] > \theta$;
            **if** $b$ hasn't been marked as visited
                mark $b$ that it belongs to cluster $i^g$;
                mark users in $b$ as members of $i^g$;
                mark $b$ as $visited$;
            **else** expand cluster $i^g$ with the cluster which cell area $b$ belongs to
            **end if**
        **else for**
    **end if**
**end for**

**Algorithm 2** Profiling

**input** group Id $g$, member Id $m^g$, residency probability matrix $\check{p}$, popularity array $p$,
**output** Clusters with assigned Id $i^g$, profile of group $\mathbb{P}_i^g$
Calculate profiled clusters using Dynamic Profiling Algorithm 1
**for** every cluster
    assign cluster Id $i^g$;
**end for**
Broadcast cluster Id $i^g$ and profile of group $\mathbb{P}_i^g$ periodically from eNodeB to MNs

**Algorithm 3** Tracking area update

**input** new cluster $i^g$, profile of group $\mathbb{P}_i^g$
**output** updated profile of group $\mathbb{P}_i^g$
**if** $m_i^g$ moves or turns phone on
  $m_i^g$ listens $i^g$, profile of group $\mathbb{P}_i^g$;
  **if** $i^g$ is not included in $\mathbb{P}_i^g$
    $m_i^g$ performs tracking area update to GLM;
  **else**
    no tracking area update;
  **end if**
**end for**

**Algorithm 4** Paging

**input** group Id $g$
**output** every cells in $\mathbb{P}_i^g$
Get profile of group $g$ from GLM
**for** every $i^g$ in $\mathbb{P}_i^g$
    **for** every cell area $c$ in $i^g$ in $\mathbb{P}_i^g$
        perform paging simultaneously through MME;
    **end for**
**end for**

### 4.5 Analysis for Signaling Traffic Overhead Analysis

In this section, we illustrate the possible savings of our GLM in signaling traffic overhead and average paging delay by comparing them with a typical ILM through theoretical analysis. Notations used in this section are summarized in Table 3.

We first show the benefit of our scheme in traffic overhead by analytically comparing the total cost of our GLM with that of a typical ILM. Here, the total cost of a location management scheme is defined as the signaling traffic overhead that is the summation of the tracking area update and paging costs. In addition, as widely accepted in previous research, the tracking area update cost is in proportion to the number of the TA boundary crossings, while the paging cost is in proportion to the size of the TAs.

Suppose the tracking area update cost for each TA boundary crossing is $C_{LU}$ and the unit cost for paging a single cell TA is $C_P$. Moreover, assume that for an individual mobile user $m$, its TA residency time $t_m$, that is the time interval between two boundary crossings, follows Gamma distribution, with density function $f_{t_m}(\cdot)$, mean $1/\lambda_m$, and variance $V_m$; and the time interval between two group calls $t_g$ follows exponential distribution with mean $1/\lambda_g$ [49]. Let us denote $Pr_m(x)$ as the probability of $x$ tracking area updates for group member $m$ between two group calls, then we have the expectation for the total number of tracking area updates/boundary crossings per call arrival using ILM as

$$E(x) = \sum_{m \in K} \sum_{x \in (0,\infty)} x \cdot Pr_m(x) \tag{4.2}$$

where

$$Pr_m(x) = \begin{cases} 1 - \frac{\lambda_m}{\lambda_g}[1 - f^*_{t_m}(\lambda_g)], & x = 0 \\ \frac{\lambda_m}{\lambda_g}[1 - f^*_{t_m}(\lambda_g)]^2[f^*_{t_m}(\lambda_g)]^{x-1}, & x > 0 \end{cases} \tag{4.3}$$

$f^*_{t_m}(\cdot)$ is the Laplace-Stieltjes Transform of Gamma random variable $t_m$ with mean $1/\lambda_m$ and variance $V_m$ [49], and it can be expressed as:

$$f^*_{t_m}(s) = (\frac{\lambda_m \gamma}{s + \lambda_m \gamma})^{\gamma},\ where\ \gamma = \frac{1}{V_m \lambda_m^2} \tag{4.4}$$

Therefore, from Equations (4.2) and (4.3), the expected number of tracking area updates between two group calls for ILM tracking area updates is

$$E(K) = \sum_{m \in K} \frac{\lambda_m}{\lambda_g} \tag{4.5}$$

Meanwhile, the paging cost for ILM is

$$\sum_{m \in K} S_m \cdot C_P \tag{4.6}$$

where $S_m$ is the size of the TA that the mobile user $m$ is located in. Therefore, the total cost per call arrival for ILM is

$$\sum_{m \in K} \frac{\lambda_m}{\lambda_g} \cdot C_{LU} + \sum_{m \in K} S_m \cdot C_P \tag{4.7}$$

On the other hand, consider the simplest GLM that the TAs for a group are determined by simply combining adjacent TAs for each group member. Therefore, the size of the group TAs is

$$\bigcup_{m \in K} S_m \tag{4.8}$$

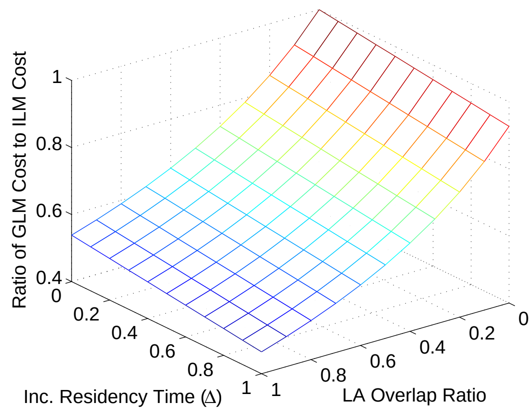


Figure 19: Comparison of Total Cost Consumed by ILM and GLM with Varied TA Overlap Ratio and Increased Residency Time $\Delta$

Notice that:

$$\bigcup_{m \in K} S_m \leq \sum_{m \in K} S_m \tag{4.9}$$

Only if $S_{m_1} \bigcap S_{m_2} = \emptyset$, where $m_1 \neq m_2$, $\bigcup_{m \in K} S_m = \sum_{m \in K} S_m$. Whereas in group applications scenarios, the MNs from one group usually have some common mobility patterns, e.g., activity area, that results in $S_{m_1} \bigcap S_{m_2} \neq \emptyset$, where $m_1 \neq m_2$. Therefore, the paging cost for GLM is smaller than that for ILM

$$\bigcup_{m \in K} S_m \cdot C_P < \sum_{m \in K} S_m \cdot C_P \tag{4.10}$$

Furthermore, it is easy to derive that:

$$\bigcup_{m \in K,} S_m \geq \forall m \in K, S_m \tag{4.11}$$

which means that the combined TAs contain TAs computed by ILM. Thus, we can derive that the residency time in the combined TAs is $t'_m = t_m + \Delta_m$, where $\Delta_m \geq 0$

is the residency time for $m$ in adjacent cell $c_l^{ij}$, where $c_l^{ij} \in L'_j$, and $c_l^{ij} \notin L_j$. Then the average residency rate for $m$ is

$$\lambda'_m \leq \lambda_m \tag{4.12}$$

For the sake of simplicity, assume the residency time for a mobile user $m$ in combined TAs follows Gamma distribution with mean $1/\lambda'_m$ and variance $V'_m$. Then the expected number of boundary crossings is

$$E'(x) = \sum_{m \in K} \sum_{x \in (0,\infty)} x \cdot Pr'_m(x) = \sum_{m \in K} \frac{\lambda'_m}{\lambda_g} \tag{4.13}$$

where

$$Pr'_m(x) = \begin{cases} 1 - \frac{\lambda'_m}{\lambda_g}[1 - f^*_{t'_m}(\lambda_g)], & x = 0 \\ \frac{\lambda'_m}{\lambda_g}[1 - f^*_{t'_m}(\lambda_g)]^2[f^*_{t'_m}(\lambda_g)]^{x-1}, & x > 0 \end{cases} \tag{4.14}$$

As $\lambda'_m \leq \lambda_m$,

$$E'(x) \leq E(x) \tag{4.15}$$

Assuming $\lambda_g = 20\ min$, $\lambda_m = 5\ min$, and the ratio of $C_{LU}$ to $C_P$ is 3, the total cost is compared in Figure 19. As shown in Figure 19, GLM can save up to $53\%$ of the total cost by reducing the expected number of boundary crossings and the paging cost and an outperform ILM in signaling traffic overhead.

### 4.6 Analysis for Average Delay

Another benefit of our proposed GLM is that it can reduce the average delay when group calls come. Intuitively, each group member is paged one by one in consecutive

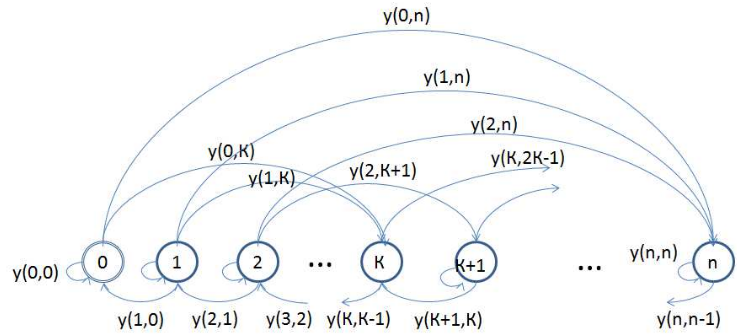


Figure 20: State transition diagram for paging requests queue in a MME using ILM

order using ILM; while all the group members that are located in the same TA can be paged at the same time by broadcasting the group Id using GLM. By doing these, GLM significantly cuts the average delay for group calls. In this section, we compare the average delay between a typical ILM and our proposed GLM and present the possible delay reduction by utilizing our GLM.

As assumed in section 4.5, the time interval between two group calls $t_g$ follows exponential distribution with mean $1/\lambda_g$. For simplicity, we only consider the average delay of $\kappa$ out of $|K|$ group members that are located in the same tracking area.

When a paging request arrives to an MME, it will be put at the end of the paging request queue. We assume that the MME processes paging requests according to their sequence in the queue, and only one paging request is processed during a time unit. Therefore, the newly arrived paging request will be severed after all the requests that arrived previously are processed [80]. Furthermore, due to the size limitation of the MME's memory, perhaps the maximum length of a paging request queue is $n$.

Without GLM, each group member will be paged in consecutive order according

$$y(i,j)_{ILM} = \begin{cases} Poisson(\lambda_g, \varepsilon, 0), & i = j+1 \\ Poisson(\lambda_g, \varepsilon, \frac{j-i}{\kappa}), & 0 = i < j < n,\ mod(j-i, \kappa) = 0 \\ Poisson(\lambda_g, \varepsilon, \frac{j-i+1}{\kappa}), & 0 < i < j < n,\ mod(j-i+1, \kappa) = 0 \\ 1 - \sum_{w=0}^{\lceil \frac{j-i-1}{\kappa} \rceil} Poisson(\lambda_g, \varepsilon, w), & i = 0,\ j = n \\ 1 - \sum_{w=0}^{\lceil \frac{j-i}{\kappa} \rceil} Poisson(\lambda_g, \varepsilon, w), & 0 \le i < j = n \\ 0, & \text{others} \end{cases} \tag{4.16}$$

$$y(i,j)_{GLM} = \begin{cases} Poisson(\lambda_g, \varepsilon, 0), & i = j+1 \\ Poisson(\lambda_g, \varepsilon, j-i), & 0 = i < j < n \\ Poisson(\lambda_g, \varepsilon, j-i+1), & 0 < i < j < n \\ 1 - \sum_{0}^{w=j-i} Poisson(\lambda_g, \varepsilon, w), & i = 0,\ j = n \\ 1 - \sum_{0}^{w=j-i-1} Poisson(\lambda_g, \varepsilon, w), & 0 \le i < j = n \\ 0, & \text{others} \end{cases} \tag{4.17}$$

to their Ids. So when a group call arrives, $\kappa$ individual paging requests will be added into the paging request queue. Since the group calls' arrival is assumed as a Poisson Process, with mean arrival rate of $\lambda_g$, the probability that there are $w$ arrived group calls, which result in $w \cdot \kappa$ paging requests in any time duration $\varepsilon$ is

$$Poisson(\lambda_g, \varepsilon, w) = \frac{(\lambda_g \varepsilon)^w e^{-\lambda_g \varepsilon}}{w!} \tag{4.18}$$

Let us denote $\varphi_i$ as the probability that there are $i$ paging requests in the queue; and that the transition matrix $Y_{ILM}$ to describes the state transition probability between states. Each element $y_{ILM}(i,j)$ in $Y_{ILM}$ represents the probability that the number of requests in the queue changes from $i$ to $j$. We show the state transition diagram in Figure 20. Each node in Figure 20 indicates a state that is $i$ request in the queue. The directed link from node $i$ to $j$ represents there is a potential state transition from state $i$ and $j$. Especially, the label $y(i,j)$ beside each link represents the transition probability of state transiting from

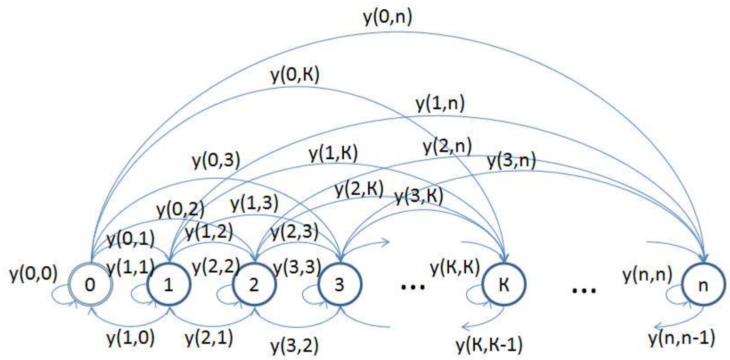


Figure 21: State transition diagram for paging requests queue in an MME using GLM

$i$ to $j$. We summarize the transition probability $y_{ILM}(i,j)$ in Equations (4.19) and (4.16).

$$y(i,i)_{ILM} = \begin{cases} Poisson(\lambda_g, \varepsilon, 0), & i = 0 \\ Poisson(\lambda_g, \varepsilon, 1), & 0 < i < n \\ & \kappa = 1 \\ 1 - Poisson(\lambda_g, \varepsilon, 0), & i = n \\ 0, & \text{others} \end{cases} \tag{4.19}$$

Denote the probability vector $\Phi$ as:

$$\Phi = [\varphi_0,\ \varphi_1, \ldots,\ \varphi_n]$$

where

$$\sum_{i=0}^{n} \varphi_i = 1 \tag{4.20}$$

When the queue system is stable, we have

$$\Phi \cdot Y_{ILM} = \Phi \tag{4.21}$$

where $Y_{ILM}$ is the transition matrix for a queueing system in an MME with an ILM.

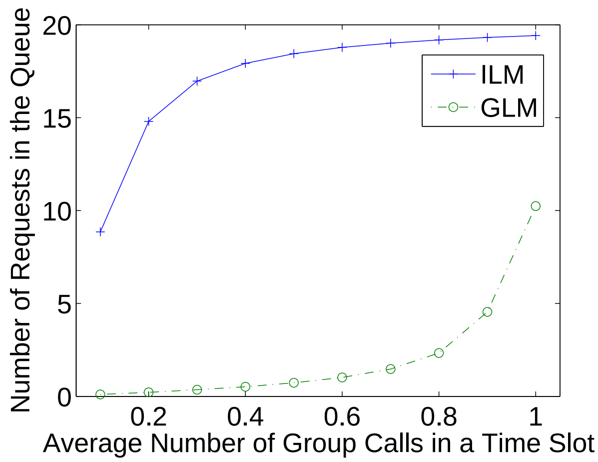


Figure 22: Number of requests in the queue with varied number of group members

By solving Equations (4.20) and (4.21) and obtaining the probability vector $\Phi$, we can estimate the number of requests in the queue as:

$$\sum_{i=0}^{n} i \cdot \varphi_i \tag{4.22}$$

On the other hand, when using our GLM, an MME pages the group members by using the group Id instead of the individual mobile user Ids, and the paging process of the mobile users in one group can be completed at the same time. As a result, we present the state transition diagram in Figure 21 and the transition probability using GLM $y_{GLM}(a, b)$ in Equations (4.23) and (4.17).

$$y(i,i)_{GLM} = \begin{cases} Poisson(\lambda_g, \varepsilon, 0), & i = 0 \\ Poisson(\lambda_g, \varepsilon, 1), & 0 < i < n \\ 1 - Poisson(\lambda_g, \varepsilon, 0), & i = n \\ 0, & \text{others} \end{cases} \tag{4.23}$$

We can compute probability vector $\Phi$ by solving Equations (4.24) and (4.25) and estimate the number of requests in the queue using Equation (4.26).

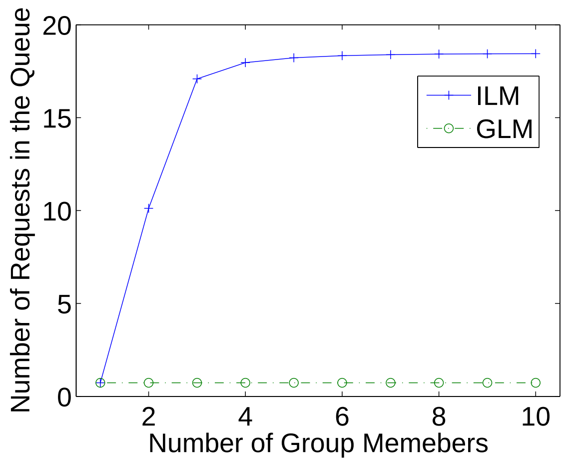


Figure 23: Number of requests in the queue with varied average call rate

$$\sum_{i=0}^{n} \varphi_i = 1 \tag{4.24}$$

$$\Phi \cdot Y_{GLM} = \Phi \tag{4.25}$$

where $Y_{GLM}$ is the transition matrix for a queueing system of an MME using GLM.

$$L_{ILM} = \sum_{i=0}^{n} i \cdot \varphi_i \tag{4.26}$$

Assume a group call arrives every two time units on average, and the MME completes the processing of each paging request in a time unit. In addition, the maximum queue length is set to $20$. The average number of requests in the paging request queue for the MMEs using both ILM and GLM are compared in Figure 22. As shown in this figure, when the number of group members increases, more requests will be generated and stay in the queue of an MME using ILM, which indicates a longer waiting time. However, this does not impact a queue of an MME using GLM. We also examine the impact of the average group call arrival frequency on the number of requests in the queue for an MME using both ILM and GLM when the number of group members is fixed to $10$ in Figure 23. As depicted in Figure 23, when group calls arrive around every $3$ time units, the queue in an MME using an ILM will be fully occupied, so that newly arrived requests will be dropped, while the queue in an MME using GLM can still handle paging requests even when the group calls arrive every time unit.

## 4.7 Evaluations with both Real Data and Data from Mobility Model

In this section, we evaluate the performance of our location management scheme with both real traces of human movement [7] and synthetic data from the human mobility model. For the human mobility model, we use a SLAW (Self-similar Least Action Walk) model [47] that generates the realistic synthetic walk traces. The SLAW expresses the regularity, as well as the spontaneity trip patterns, in the daily mobility of humans. The main heuristic algorithm called the LATP (Least Action Trip Planning) generates heavy-tail flights on top of fractal waypoints. People plan their trips over known destinations (view waypoints as destinations) in a gap-preserving manner where they visit the nearby destinations first before visiting farther destinations. We focus on observing the number of tracking area updates and paging areas, in order to investigate the impact of profiling and weight on the profile. In addition, we also observe the influence of self-similarity in the users' movement patterns for location management.

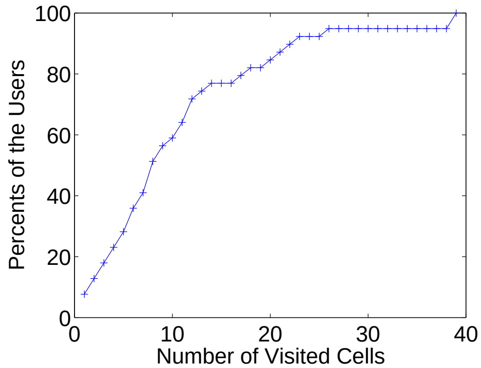


(a) Number of cells visited by users in a day

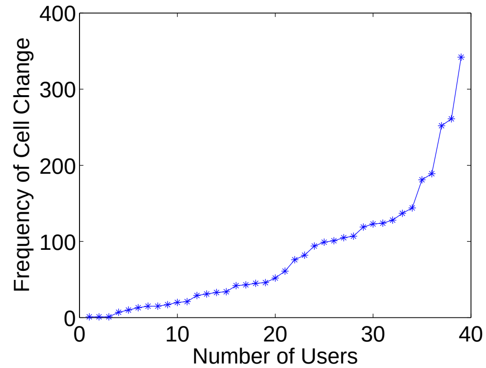


(b) Frequency of cell change in a day

Figure 24: Data analysis for real trace

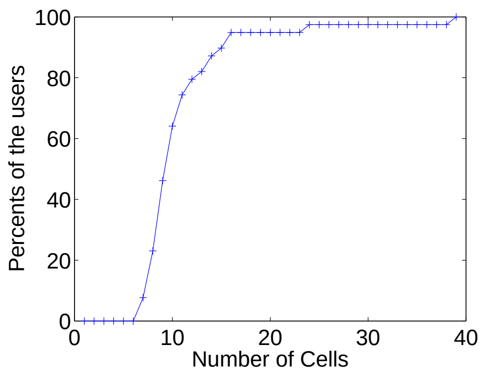


(a) Number of cells visited by users in a day

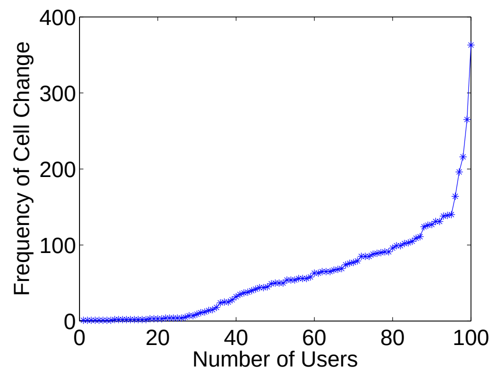


(b) Frequency of cell change in a day

Figure 25: Data analysis for SLAW data

### 4.7.1 Data sets

The users move around in a 15000 by 15000 meter area that can be representative of a large campus or city. The entire topology consists of 500 cells. Detailed settings for both data are shown in Table 4.

For the SLAW data, we set 5000 waypoints where the users selected several points

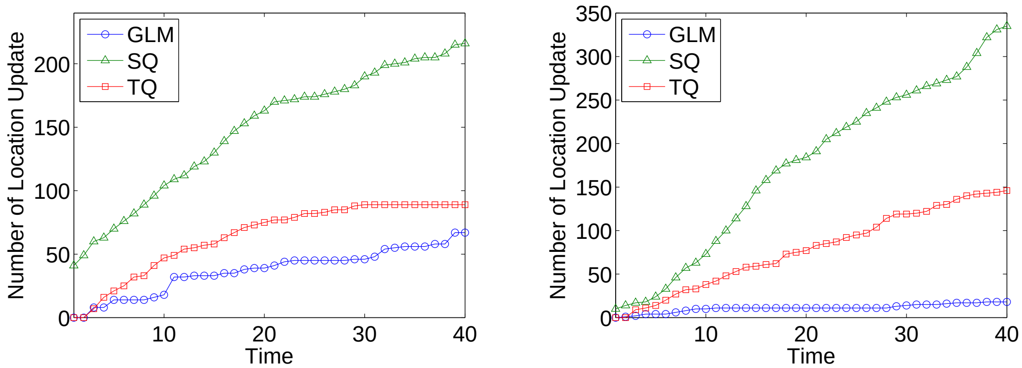


(a) Real trace (b) SLAW data

Figure 26: Comparison of number of tracking area updates ($\alpha$ = 0.9, $\theta$ = 0.3, $h$ = 0.75)

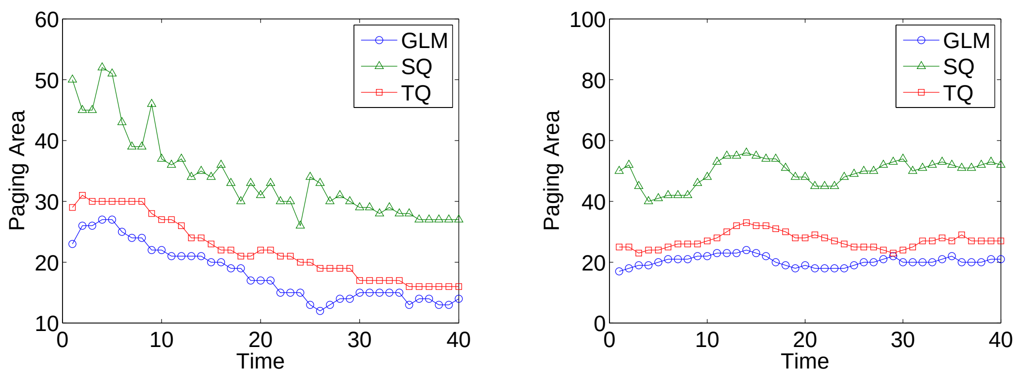


(a) Real trace (b) SLAW data

Figure 27: Comparison of the sizes of paging area ($\alpha$ = 0.9, $\theta$ = 0.3, $h$ = 0.75)

to pause during their movements. The pause time followed truncated power law distribution in the range of 30 seconds to a maximum of 6 hours.

From the real trace and SLAW data, we have several observations. We observed that the users cross the cell boundary frequently; however, movement occurs in a small number of cells. From the real trace, 50 percent of the users visited fewer than 10 cells and 80 percent of them visited fewer than 20 cells. From the SLAW data, 70 percent of the

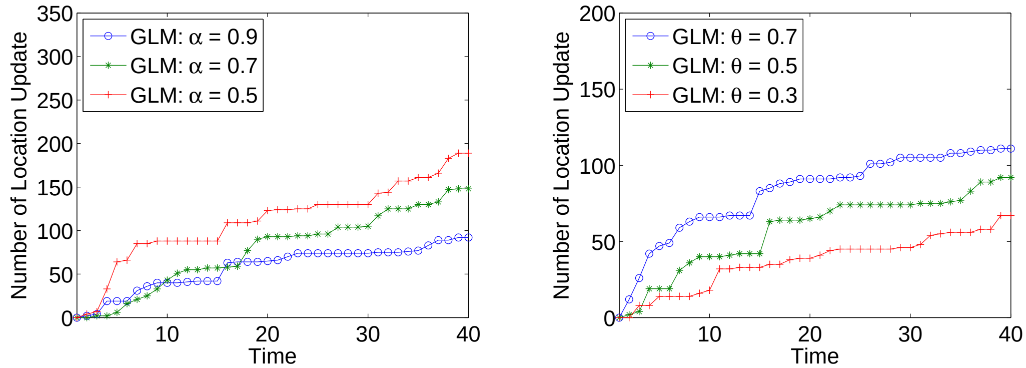


(a) varied $\alpha$ (b) varied $\theta$

Figure 28: Impact of the GLM parameters on number of tracking area updates (Real trace)

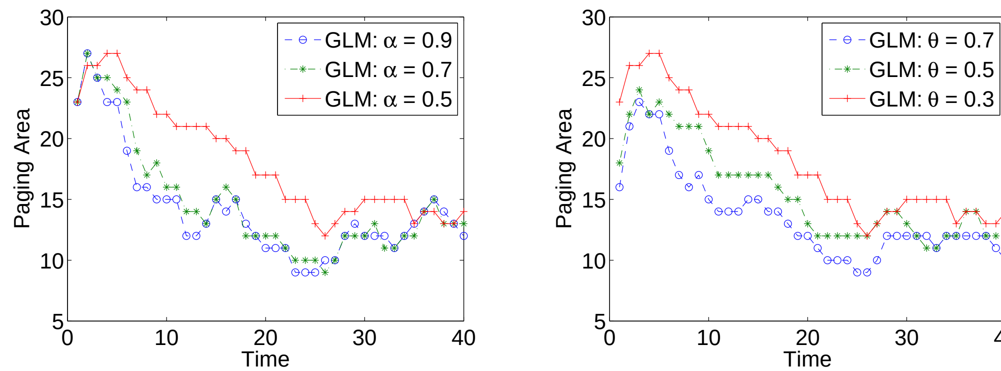


(a) varied $\alpha$ (b) varied $\theta$

Figure 29: Impact of the GLM parameters on the size of paging area (Real trace)

users traveled within 10 cells and 95 percent of them traveled within 20 cells. However, the average number of cell changes for all users in a day was 58 times for the real trace and 71 times for the SLAW data. Additionally, from the number of cell changes, we determined the time intervals of group profiling as 15 minutes for the real trace and 30 minutes for the SLAW data.

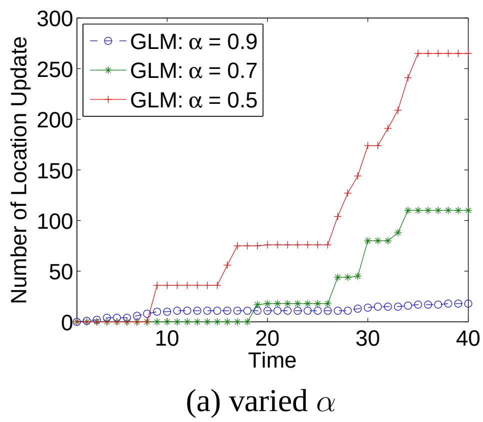


Figure 30: Impact of the GLM parameters on the number of tracking area updates (SLAW data)

#### 4.7.2 Experiments

In this subsection, we discuss the experimental results obtained from the varied parameters to the number of tracking area updates and the size of the paging area. First, we compare our GLM with both spatial quantization (SQ) [65] and temporal quantization (TQ) [65]. SQ groups the spatial adjacent cells into a cluster and performs tracking area updates at the cluster level. TQ groups the set of consecutive cells visited by the MNs and reports patterned movement to the network. Compared to our result, SQ showed very similar results to our algorithm with a high threshold that generated a small TA. TQ showed a better performance at the beginning, but it reached a similar amount of tracking area updates as time went on. With real trace, the cumulated average number of tracking area updates of the GLM showed a similar result to TQ, which is described in Figure 26(a), and the GLM showed a better result with the SLAW data in Figure 26(b). In addition, the size of the paging area of the GLM was compared with both SQ and TQ

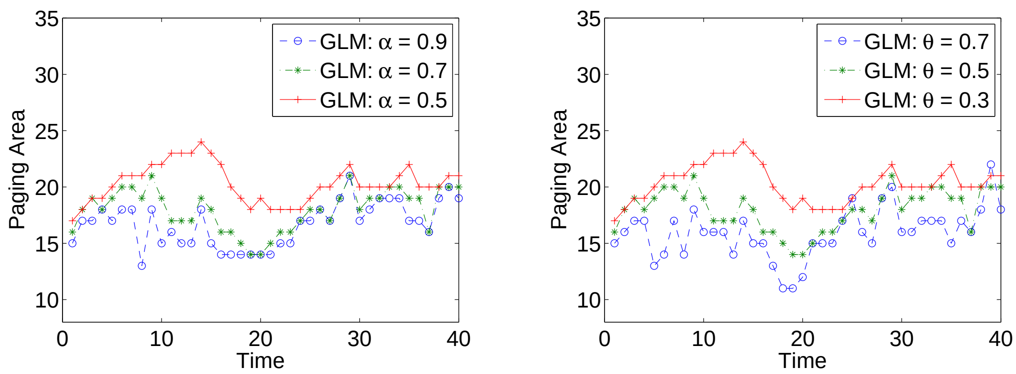


(a) varied $\alpha$ (b) varied $\theta$

Figure 31: Impact of the GLM parameters on the size of paging area (SLAW data)

in Figures 27(a) and 27(b), and those showed that the GLM has a smaller look up area for both the real trace and synthetic data.

Next, we took a closer look at the impact of weight ($\alpha$) and threshold ($\theta$) on the GLM that is depicted in Figures 28, 29, 30, and 31. We observed that using a history of the users' movements resulted in better performance in a low number of tracking area updates and a smaller size of the paging area from Figures 28(a), 29(a), 30(a), and 31(a), as well. Impact of $\theta$ is shown in Figure 28(b), 29(b), 30(b), and 31(b). Since the low-$\theta$ generated a smaller TA, the GLM performed the smallest number of location updates with the low-$\theta$. In other words, we observed that the size of the paging area was the largest with the low-$\theta$. While the difference in the size of the paging area was smaller, the difference in the number of tracking area updates was larger among varied $\theta$. Furthermore, the cost of tracking area updates was three times larger than the cost of the paging area [75,79,80]. From this observation, we can infer that the total cost of location management is lower for low-$\theta$ with our experiment's settings.

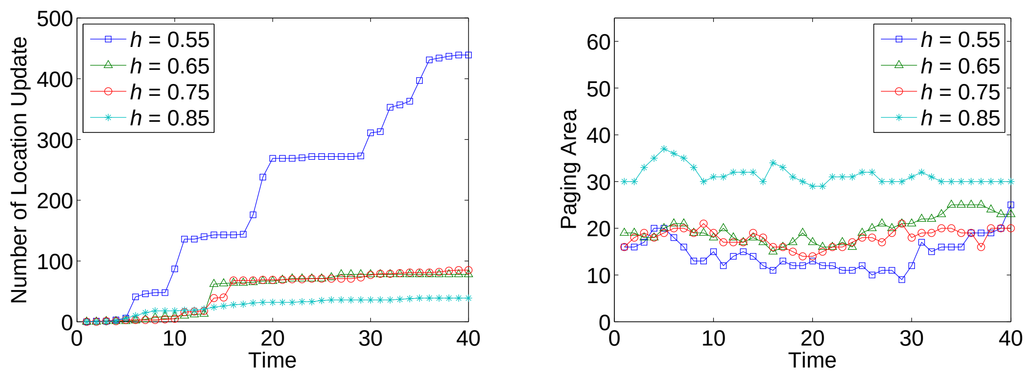


(a) Tracking area update

(b) Paging area

Figure 32: Impact of data characteristic using varied hurst parameters ($\alpha$ = 0.9, $\theta$ = 0.5, SLAW data)


Figure 33: Worst and best cases of paging: Right before and after dynamic profiling

We also varied one of the characteristics of the user's movements self-similarity that is the hurst parameter (0.5 $< h <$ 1.0) in [47]. The hurst parameter controls the degree of self-similarity of the user's movement patterns. We observed that the number of tracking area updates was decreasing while the self-similarity was increasing in Figure 32(a). This is because our method considered the geographical information while we profiled the MN's movement.

Finally, we examined the paging success rate with varied $\alpha$ and $\theta$. Figure 33 depicts the best case and worst case paging scenarios. In our simulation, since we have the data that reports the users' locations every 30 seconds, the best case paging was 30 seconds later than the cluster regeneration and the worst case paging was 30 seconds before the cluster regeneration. Table 5 shows the average paging success rate for each threshold. We observed $\theta$ between 0.3 and 0.5 showed a high success rate. Also, we observed that the paging success rate was higher while we used higher $\alpha$ in order to give more incentive on the history of the users' movement patterns.

#### 4.7.3 Cost evaluation for location management

In this section, we evaluate the location management cost that consists of two components: the tracking area update cost and paging cost. Also, we observe the effect of the hurst parameter that can vary the self-similarity of the mobile users' movement pattern on the cost of location management.

In order to study the location management cost and understand factors that can impact the cost, we used the average number of tracking area updates and the size of the paging area that we obtained in section 4.7.2. From the result of section 4.7.2, we already know that both the tracking area update cost and paging cost can be effected by the size of the TAs and the self-similarity of the mobile user's movement. The mobile user's movement can be classified as below.

- $M_m^{cell}$: average number of movements of user $m$ across cell boundary
- $M_m^{TA}$: average number of movements of user $m$ across the TA boundary
- $M_m^{P}$: average number of movements of user $m$ across the TA boundary within a group profile

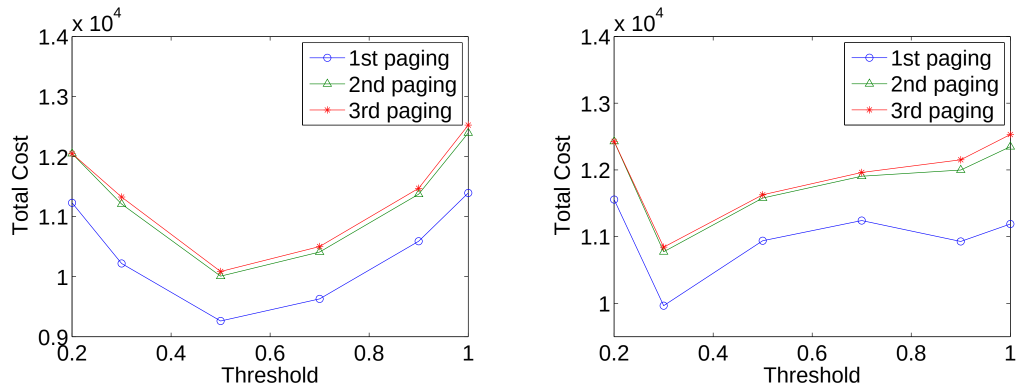


(a) Real trace (b) SLAW data

Figure 34: Total cost with varied threshold

An mobile user will not perform a tracking area update for a cell boundary crossing, $M_m^{cell}$ and a TA boundary crossing within a group profile, $M_m^P$. Our expected average number of location updates can be presented as $M_m^{TA}$-$M_m^P$. The number of tracking area updates is considerably related to the self-similarity of the mobile user's movement and size of the TA. Let $S_m(\theta)$ be a size of the TA where $m$ is located. Then, we can describe the total cost of location management as below.

$$C_{Total} = \sum_{m \in K} (M_m^{TA} - M_m^P) * C_{LU} + \sum_{m \in K} S_m(\theta) * C_P \tag{4.27}$$

We first observed the location management cost of the real data and SLAW data. Figure 34(a) depicts the total cost with real trace and Figure 34(b) shows the total cost with SLAW data. The lowest total cost is shown with threshold 0.5 in real trace and 0.3 in the SLAW data. From this result, we recognized the effect of the size of the TA, $S_m(\theta)$, on the location management cost.

However, the location management cost can be effected by self-similarity. We

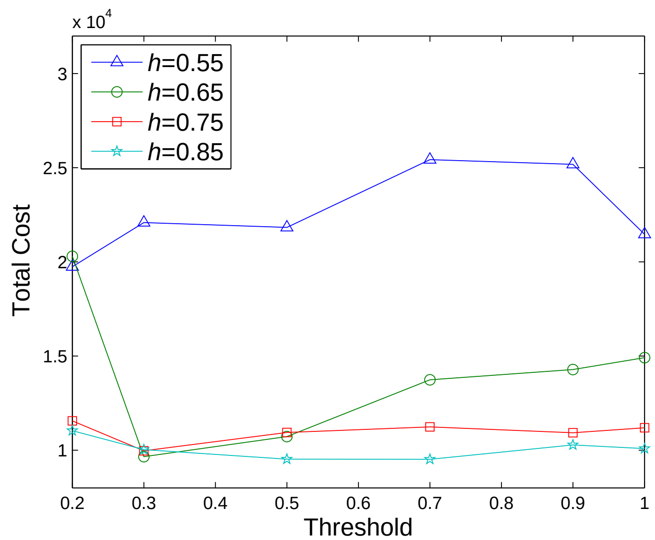


Figure 35: Total Cost with varied Hurst parameter values ($h$)

evaluated the total cost with the data that varied the hurst parameter on the SLAW data. In Figure 35, we observed that the total cost is lower when we have higher self-similarity in the users' movement patterns. Additionally, threshold 0.3 has the lowest total cost for hurst 0.65 and 0.75, but threshold 0.5 shows the lowest total cost for hurst 0.85. Thus, we suggest the range of threshold $\theta$ that decides the size of the TA rather than an optimal threshold.

### 4.8 Summary

The cellular networks are evolving with NFV architecture. We proposed a group location management scheme as a virtualized network function in cellular networks for an improved group application service. The presence of the virtualized group management function efficiently facilitates the group location management task and enables a provider to handle a large number of members and groups that otherwise would be impossible in practice.The group profiling algorithm dynamically updates its group members' locations information with clusters of cells or tracking areas that can be of arbitrary shapes. We validated the efficiency of the proposed scheme with theoretical analyses as well as experiments. The theoretical analyses showed the total signaling traffic cost and significant reduction of average delay. As for the experiments, we used both real traces of human movements and synthetic human mobility data for the tracking area update and paging costs. Moreover, we investigated the impact of the parameter that describes the self-similarity of the human walk and suggested the range of the threshold that decides the size of the TA. To the best of our knowledge, our work is the first to address the issue of location management for group applications.

There are related challenges that need to be addressed in the future. The benefit of the proposed architecture can be further substantiated with the development and evaluation of a group call signaling protocol that we plan to address in the near future. Also, there is no human group mobility model at the moment, and it would be useful for evaluations of schemes for group applications. That will also enable us to perform a detailed theoretical analysis of the proposed group location management scheme.

Table 3: Explanation of additional notations used in analysis

| Notation | Explanation |
|---|---|
| $u_j^i$ | Cluster $j$ in group $i$ |
| $C_P$ | Unit cost of paging a single cell |
| $C_{LU}$ | Unit cost of a single tracking area update operation |
| $Pr_m(x)$ | Probability of $x$ numbers of boundary crossings for a mobile user $m$ when using ILM |
| $Pr'_m(x)$ | Probability of $x$ numbers of boundary crossings for a mobile user $m$ when using GLM |
| $S_m$ | Size of TA where a mobile user $m$ is located |
| $\lambda_g$ | Average group call rate |
| $t_g$ | Time interval between two group calls that follows Poisson distribution |
| $t_m$ | TA residency time for a mobile user $m$ that follows Gamma distibution |
| $\lambda_m$ | Average cell residency rate for a mobile user $m$, which is also the mean value of $t_m$ |
| $V_m$ | Variance of $t_m$ |
| $f_{t_m}(\cdot)$ | Density function of $t_m$ |
| $f^*_{t_m}(\cdot)$ | Laplace-Stieltjes Transformation of Gamma random variable $t_m$ |
| $\kappa$ | Number of group members in an TA |
| $n$ | Maximum length of the paging request queue |
| $\varphi_i$ | Probability that there are $i$ paging requests in the queue |
| $Y_{ILM}$ $Y_{GLM}$ | Transition matrix for paging process using ILM/GLM scheme |
| $y(i,j)_{ILM}$/ $y(i,j)_{GLM}$ | Element in matrix $Y_{ILM}$/$Y_{GLM}$ that represents the probability that the number of requests in the queue changes from $i$ to $j$ |
| $\Phi$ | Set of $\varphi_i$, where $\varphi_i$ is the probability that there are $i$ paging requests in the queue, and $i \in [0, n]$ |

Table 4: Data sets used

| Parameters | Real Trace [7] | SLAW Data [47] |
|---|---|---|
| Number of users | 39 | 100 |
| Duration | 10 hours | 24 hours |
| Interval of data | 30 seconds | 60 seconds |
| Subgroup Regeneration | every 15 minutes | every 30 minutes |

Table 5: Impact of threshold on average paging success rate

| | Real Trace | | SLAW Data | |
|---|---|---|---|---|
| Threshold | Best | Worst | Best | Worst |
| 0.3 | 0.8910 | 0.8821 | 0.9166 | 0.9141 |
| 0.4 | 0.9038 | 0.8962 | 0.9244 | 0.9231 |
| 0.5 | 0.8949 | 0.8840 | 0.9167 | 0.9141 |
| 0.7 | 0.8853 | 0.8763 | 0.8654 | 0.8558 |
| 0.8 | 0.8821 | 0.8705 | 0.8545 | 0.8429 |
| 0.9 | 0.8833 | 0.8712 | 0.8494 | 0.8397 |

# CHAPTER 5

# ENODEB CONTROL WITH SDN AND NVF FOR ENERGY SAVING

Limitations of cellular networks arise from vendor-specific configuration interfaces and communications through complex control plane protocols [43]. As shown in Figure 36, a Radio Resource Control (RRC) such as mobility management, paging control, and security management are currently included in each eNodeB operation [42].

An emerging network architecture, SDN, simplifies network management and enables researchers to innovate networking and communication by decoupling the control plane from the data plane. By introducing the concept of SDN into cellular networks, the control plane of eNodeB moves to a separated controller to enable global control and efficient management in cellular networks. We suggest decoupling the network function that focuses on optimizing energy consumption of eNodeB.

In this section, we present our proposed architecture, Siesta, in cellular networks and cell management algorithms for energy efficient software-defined eNodeB control.

## 5.1 Siesta Architecture

We note that our proposed architecture is based on LTE or LTE-Advanced. The eNodeB in LTE and LTE-Advanced is responsible for radio resource allocation, handover, and paging control. [43] discusses the lack of central control of eNodeBs results in inefficient radio resource control.

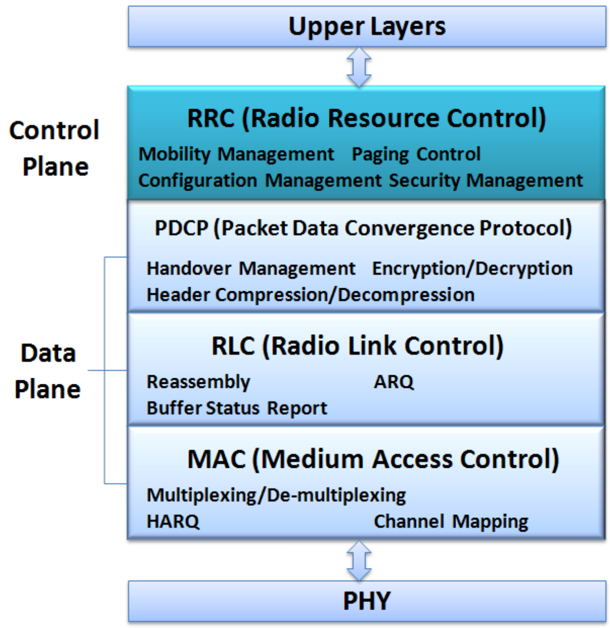


Figure 36: eNodeB (LTE, LTE-A) protocol stack with combined control and data planes

We suggest to virtualize the network function of the eNodeB power control with placing Siesta above the network controller. The Siesta module handles the eNodeB power control decisions such as sleep and wake-up modes, and assists user mobility and handover process. The detailed functionality of the Siesta in Figure 37 is as follows:

***a) eNodeB power control:*** The eNodeB power mode is defined by the Siesta through a cell operation algorithm. For power mode decisions, the history of previous power consumption and network elements information is considered. The energy-aware cell management algorithm gives a decision on the eNodeB status and user coverage. The detailed algorithm is presented in Section 5.4.

***b) Mobility management:*** Depending on the eNodeB status decision, some of the users

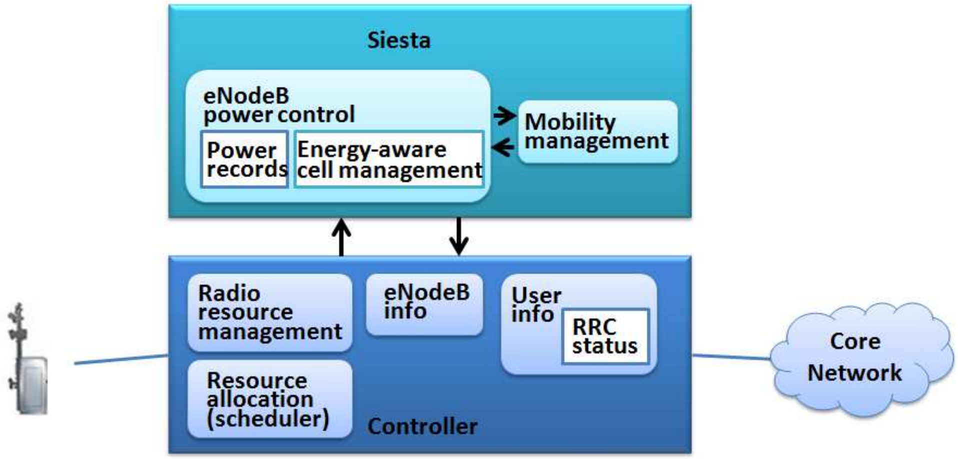


Figure 37: Siesta, a virtualized network function on SDN

will need to perform a handover. Mobility management includes establishment, configuration, and a radio bearer maintenance between eNodeB and user.

Other RRC and information remains in the controller such as the establishment of the RRC connection and security functions. The Siesta communicates with the controller to obtain the network-wide view of the cellular network.

Figure 38 shows the view of the cellular network with Siesta. Compared to the current LTE cellular network architecture illustrated in Figure 39, a controller with Siesta is added without changing the core network. The controller is mainly responsible for management of eNodeBs, users, and mobility information. With migrating the RRC from eNodeB to the controller, it simplifies the role of eNodeB and makes it easier to innovate in resource allocation and management. Figures 40 and 41 illustrate the differences in control and data flows between network elements due to the changed element in charge of the RRC. The major difference is the removed control plane among eNodeBs, such as an inter-handover and paging, since the eNodeBs are now mainly responsible for the data plane. Information handled by Siesta through the controller is as follows:

- Set of eNodeBs with id $i$: $\{e_i | i = 1, ..., k\}$
- Traffic load of $e_i$: $T^i_{curr}$,current traffic, $T^i_{min}$, minimum threshold of $e_i$, $T^i_{max}$, maximum threshold of $e_i$.
- Users' spatial information: id $i$ of current serving eNodeB and neighbor eNodeBs for each user.
- Total energy consumption of a network in duration $\tau$: $P(\tau)$

The necessary global information includes the traffic load and coverage range information of each eNodeB and spatial information of the users. The information of current and possible serving eNodeB will be used to identify user coverage for different eNodeB status. With network-wide information and virtualized control, the network with Siesta can simplify the management of eNodeBs.

## 5.2 Energy Control with Siesta

The operation of eNodeB can be divided into several mode: sleep mode, when no user is served and eNodeB is in sleep; active mode, when the eNodeB serves the users; increased mode when the eNodeB supports more users for their neighbor eNodeBs. Let us denote the power consumption of eNodeBs by $P_{sl}$, $P_{ac}$, and $P_{in}$ respectively. We use the following power consumption model for the different modes of eNodeB. The active mode power model is simplified from [14]. The power level of eNodeB $i$ is determined by

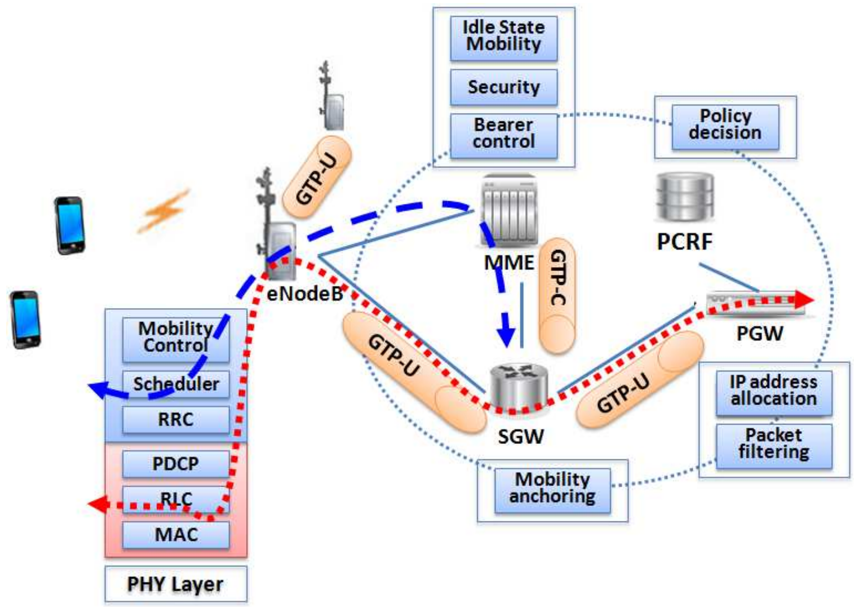


Figure 38: Architecture of current LTE cellular networks

$$p_i = \begin{cases} P_{ac} + \Delta_p \cdot N_{in} \cdot P_t \cdot C, & \text{increased mode;} \\ N_{sector} \cdot P_t \cdot C, & \text{active mode;} \\ P_{sl}, & \text{sleep mode.} \end{cases} \quad (5.1)$$

where $N_{sector}$ represents the number of sector of eNodeB and number of power amplifier per sector is assumed as a constant. $P_t$ presents the transmission power and the energy for cooling and power supply is simplified as a constant value $C$. $\Delta_p$ is the percentage of power increase to cover more users and $N_{in}$ is the number of sector that increased power in increase mode. We assumed the linear power increase in our evaluation from the observation of [16] for both active and increased mode.

Our objective is to minimize energy consumption of a network by coverage area optimization with requirement of covering all users. Consider a cellular network with

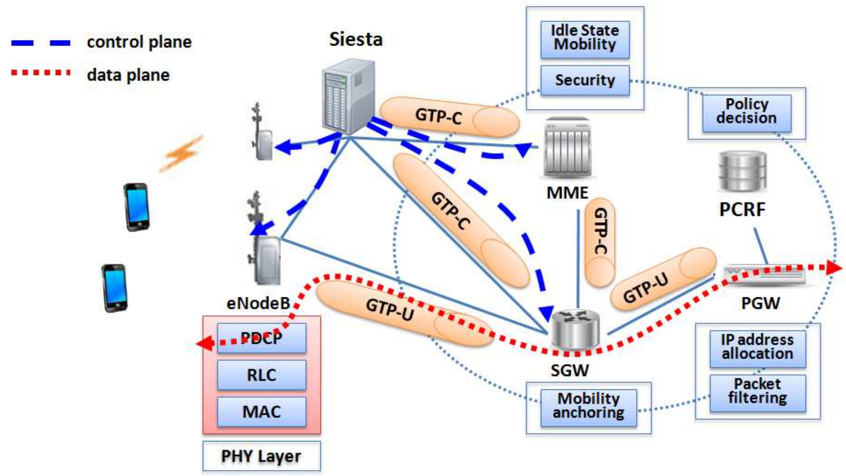


Figure 39: Architecture of Siesta

*k* eNodeBs and *n* number of users. Siesta computes the coverage optimization every $\tau$ times. While the current mobile users select their target eNodeB based on the signal strength from the eNodeBs, Siesta determines the user coverage with a set of selected eNodeBs in our proposed method.

Let us denote $U$ as a set of users $U = \{u_1, u_2, ..., u_n\}$, and $E$ as a set of eNodeBs $E = \{e_1, e_2, ..., e_k\}$. The Siesta will optimize the association between eNodeB and users every $\tau$ period. The energy consumption of *k* number of eNodeBs can be expressed as:

$$P(\tau) = \sum_{i=1}^{k} p_i(\tau) \cdot a_i(\tau) \cdot \tau \tag{5.2}$$

Here, $p_i$ is the power consumption of eNodeB $i$, and $a_i$ is an indication function that is set to 1 when eNodeB $i$ is in active or increased mode at the $\tau$ duration; otherwise, $a_i$ is 0. Note that sleep mode is also considered as on because it consumes a certain

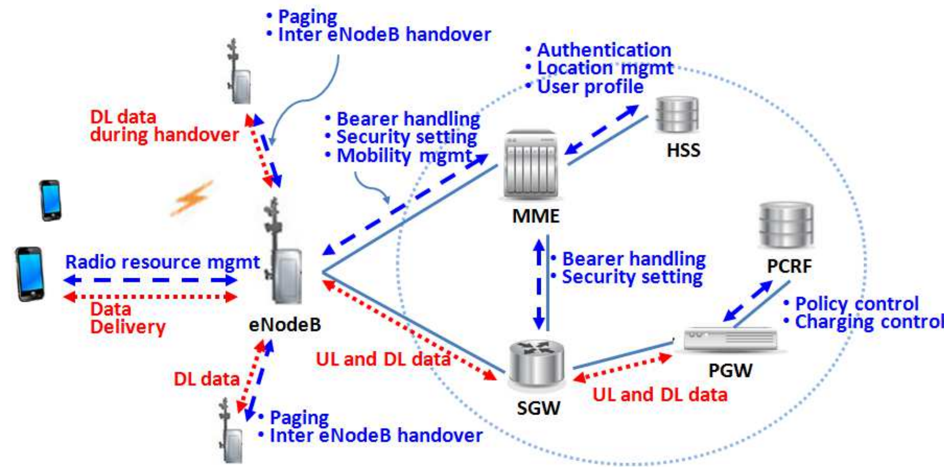


Figure 40: Control and data flows among network elements of current LTE cellular networks

amount of energy, $P_{sl}$.Therefore, $a_i$ can be expressed as:

$$a_i(\tau) = \begin{cases} 1, & \text{eNodeB } i \text{ is } \textit{on}; \\ 0, & \text{Otherwise}. \end{cases} \tag{5.3}$$

During an eNodeB status update, Siesta will consider the number of users under the eNodeBs and select eNodeBs and their status according to the cardinality of each eNodeB. Then we have the set of selected eNodeBs $E' = \{e_1, e_2, ..., e_k\}$

$$\begin{aligned} &\min P(\tau), \\ \text{subject to } &\sum_{u \in U} u_j = n, \\ &a_{i \in E'} \in \{0, 1\} E' \subseteq E. \end{aligned} \tag{5.4}$$

Here, $u_j$ indicates the user $j$ that equals 1 when the user has an association with a certain eNodeB at the $\tau$ duration; otherwise, $u_j$ equals 0.

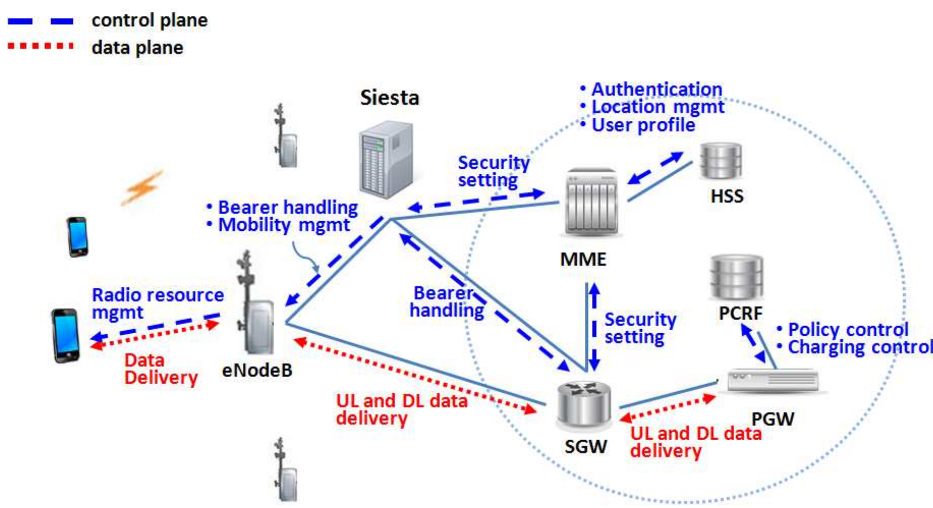


Figure 41: Control and data flows among network elements of Siesta

$$u_j(\tau) = \begin{cases} 1, & \text{user } j \text{ is \textit{associated} with an eNodeB;} \\ 0, & \text{Otherwise.} \end{cases} \tag{5.5}$$

### 5.3 Energy-aware Cell Management Algorithm in Siesta

We now present our energy-aware cell management algorithm that gives a better decision on handover and eNodeB status for energy saving. In our proposed algorithm, the Siesta will find out the serving eNodeB for each user. Also, with centralized information in the controller, we check the users' spatial distribution and the status of the eNodeBs beyond the surrounding neighbor eNodeBs to maximize the sleeping eNodeB.

We develop our algorithm by applying the set cover problem. Since the set cover problem is known as an NP-hard problem, we developed a heuristic algorithm based on [25] that can minimize the set of active eNodeBs. Our proposed cell management

Table 6: Explanation of Notations used in Cell Management Algorithm

| Notation | Explanation |
|---|---|
| $e_i$ | eNodeBs with id $i$ |
| $u_j$ | Users with id $j$ |
| $E$ | Set of eNodeBs, $E = \{e_1, e_2, ..., e_k\}$ |
| $U$ | Set of users, $U = \{u_1, u_2, ..., u_n\}$ |
| $E'$ | Set of active eNodeBs |
| $T^i_{curr}$ | Current traffic of eNodeB $i$ |
| $T^i_{min}$ | Minimum traffic threshold of eNodeB $i$ |
| $T^i_{max}$ | Maximum traffic threshold of eNodeB $i$ |
| $p_i$ | Energy consumption of eNodeB $i$ |
| $a_i$ | Indication function of eNodeB $i$ status |
| $c_j$ | Indication function for association between user $j$ and eNodeB |
| $P(t)$ | The total energy consumption at time $t$ |

algorithm includes two parts: initialization and decision making. Initialization algorithm checks current status of eNodeB and identifies covered users for each eNodeB to initiate cell management algorithm. Decision making part decide the mode for eNodeB such as sleep, active, and increased. The notations used in cell management algorithm is explained in Table 6.

Cell management algorithm initiated by change of the current current status of eNodeBs and users as described in algorithm 5. When a certain eNodeB reaches threshold $T^i_{min}$ or $T^i_{max}$, Siesta identifies the covered users for each eNodeB, $e_i$, with different statuses such as the power increased mode, active mode, and sleep mode.

For example, if the set of covered users of eNodeB $a$, $b$, and $c$ is

$$e_a = \{u_1, u_2, ..., u_q\}$$

**Algorithm 5** Initialization of cell management

**input** user set $U = \{u_1, u_2, ..., u_n\}$, eNodeB set $E = \{e_1, e_2, ..., e_k\}$, traffic thresholds $T^i_{curr}$, $T^i_{min}$, and $T^i_{max}$
**output** a set of selected eNodeBs to be active, $E'$
**if** $(\exists\, T^i_{curr} \leq T^i_{min})$ or $(\exists\, T^i_{curr} \geq T^i_{max})$ **then**
  $E' \leftarrow \emptyset$;
  identify covered users for each $e_i$ with different status;
  sort $E$ in descending order according to number of covered users;
**end if**
**return** sorted eNodeB set, $E$

$$e_b = \{u_1, u_2, ..., u_p\}$$

$$e_c = \{u_1, u_2, ..., u_r\}$$

Then, sort the eNodeB set in descending order according to the cardinality of each status. The cardinality of the eNodeBs is $|e_b| = p, |e_a| = q, |e_c| = r$ with $p \leq q \leq r$. The sorted eNodeB set is

$$E_{sorted} = \{(e_b, e_a, e_c)\}$$

From the returned sorted set of eNodeBs, algorithm 6 selects an eNodeB that has the highest number of uncovered users and add to the set $E'$. We repeat this step until all the users in the set $U$ are covered by set $E'$. However, if all the users under a certain eNodeB are covered by other sets then we remove the eNodeB from the selected set $E'$.

The cost of covering users can be expressed as:

$$c_i = w(e_i)/|e_i \cap R| \tag{5.6}$$

**Algorithm 6** Energy-aware cell management

**input** sorted eNodeB set, $E$
**output** a set of selected eNodeBs to be active, $E'$
**while** $E'$ does not cover all users in $U$
    select a $e_i$ with the highest number of uncovered users;
    $E' \leftarrow E' \cup e_i$;
    **if** all users under $e_i$ covered by other sets **then**
        remove the set $e_i$ from $E'$;
    **end if**
    calculate cost for $c_i = w(e_i)/|e_i \cap R|$;
**end while**
**return** a set of selected eNodeBs, $E'$

where $w(e_i)$ is the weight of the eNodeB $i$ and $R$ is the set of users that are uncovered when $e_i$ is picked. The weight of eNodeB, $w(e_i)$, can vary according to the type and power level of eNobeB.

Finally, the algorithm returns the minimum set of active eNodeBs, $E'$, that covers all the users. We achieve our goal that minimizes the power consumption with a minimum set of active eNodeBs in a cellular network through the Siesta energy-aware cell management algorithm.

We have extended our energy-aware cell management algorithm with recognizing the eNodeB sectorized antenna. Our proposed sector-based cell management algorithm described in algorithm 7 has considered 3 sector macro eNodeB based on the study of [14]. With sector-based cell management algorithm we aim to decrease the unnecessary use of energy from the sector where no users are laid over.

**Algorithm 7** Sector-based cell management

**input** sorted eNodeB set, $E$
**output** a set of selected eNodeBs to be active, $E'$
**while** $E'$ does not cover all users in $U$
    select a $e_i$ with the highest number of uncovered users;
    define the sector information(ID) for each user under $e_i$ based on users' spatial information;
    $E' \leftarrow E' \cup e_i(s_1, s_2, s_3)$;
    **if** all users under $e_i$ covered by other sets **then**
        remove the set $e_i$ from $E'$;
    **end if**
    calculate cost for $c_i = w(e_i)/|e_i \cap R|$;
**end while**
**return** a set of selected eNodeBs, $E'$

This algorithm also uses the sorted eNodeB set that is a returned value from algorithm 5 as a input and select a $e_i$ according to the number of uncovered users until all the users are covered. For sector-based cell management, the Siesta defines the sector ID for each user under $e_i$ based on users' spatial information. The important part of the algorithm is that the $e_i$ includes sector status information to add to the set $E'$ as following.

$$E' \leftarrow E' \cup e_i(s_1, s_2, s_3) \tag{5.7}$$

where $s_1$, $s_2$, and $s_3$ indicates the three sector status that equals 1 when the sector of $e_i$ is active; otherwise, the sector status equals 0.

As for the complexity of our proposed algorithm, it costs $O(n)$ time to determine whether all the users in set $U$ are covered or not, where $|U|$ is equal to $n$. A minimum subset $E'$ can be found in $O(\log k)$, where there is $k$ number of eNodeBs in set $E$. Consequently, the total time complexity of our algorithm is $O(n \log k)$.

## 5.4 Siesta Cell Management

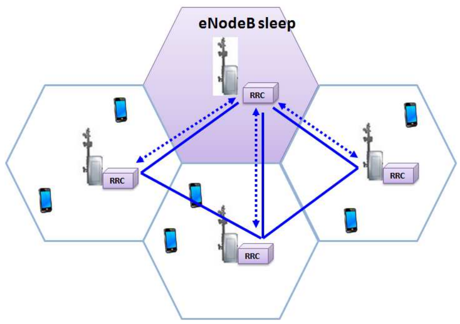


(a) SLAKE [60]

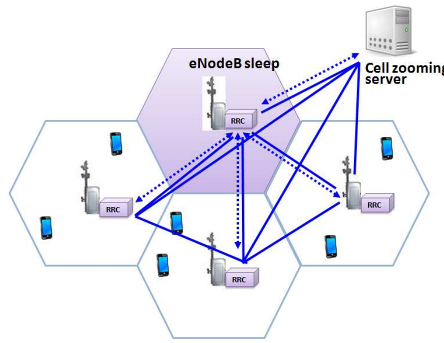


(b) Cell zooming [59]

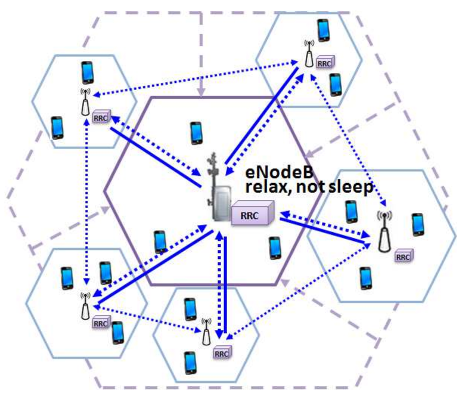


(c) Relax [33]

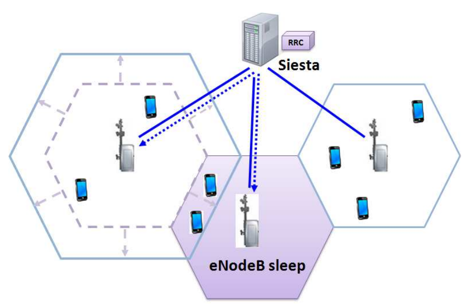


(d) Siesta

Figure 42: Existing eNodeB sleep and wake-up schemes for energy saving (solid line: control plane, dotted line: control message exchange for eNodeB sleep)

A global view of cellular networks provides benefits not only in power saving but also in a control procedure. First, we describe the advantage in the control message exchange for RAN. Then, the reduced control message for the core network during the handover procedure are compare to the current LTE cellular networks is illustrated. Finally, we present the energy saving scenario that increases the number of sleeping eNodeBs with the view beyond the neighbor eNodeBs.

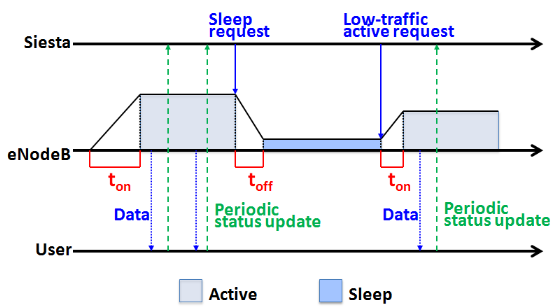

(a)Control message exchange

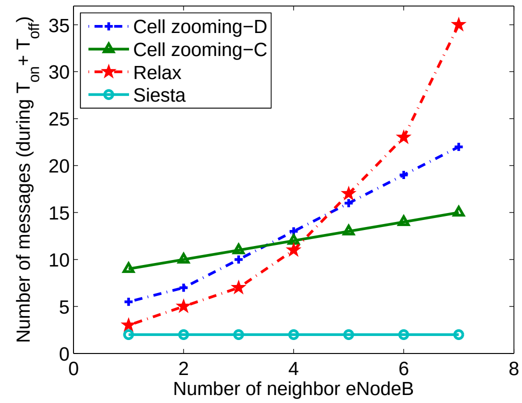

(b)Comparison of message exchange

Figure 43: Control message of Siesta for eNodeB status change

### 5.4.1 Control Message Comparison

We first explain the control message exchanges of prior eNodeB sleep and wake-up algorithms. Then we compare the number of message exchange with Siesta during the transition of eNodeB status.

***Description of previous studies:*** A distributed algorithm *SLAKE* [60] that communicates with the only neighbors for eNodeB's switch on-and-off and zooming is illustrated in Figure 42(a). In this algorithm, each eNodeB has an RRC procedure so that the decision for the sleep and wake-up mode is made by eNodeB itself after contact with its neighbor nodes. Similarly, distributed schemes are proposed in [40, 67]. Although these methods suggest different algorithms, the eNodeB still needs to contact all neighbors for a decision. A centralized algorithm *Cell Zooming* [59] that introduces a new component and corresponding functionalities is described in Figure 42(b). For central control there is a cell zooming server that stores network information such as user requirements and channel state information. The cell zooming server uses this information in order to make a decision for network operations such as eNodeB cooperation. Despite the support of the server, the eNodeB needs to exchange the control message with neighbors since RRC management remains in each eNodeB. Another method in Figure 42(c) that uses relay stations and reduces the power instead of putting the eNodeB in sleep mode, named *Relax* is presented in [33]. In this method, they use the information of each user such as the distance from a certain eNodeB to the users and energy consumption between a certain eNodeB and users. In order to reduce the coverage of eNodeB which has low traffic, they place relay stations (small cells) to cover the remaining users. Placement of relay stations also causes communication overhead among eNodeB and the relation stations.

In Siesta, Figure 42(d), RRC is moved from eNodeB to the controller and Siesta, and eNodeBs have been simplified. The decision for eNodeBs status is made by Siesta and the control messages among eNodeBs are removed.

***Control message during transition time:*** Control messages among Siesta, eNodeB, and user are described in Figure 43(a). Users and eNodeBs update their status periodically, and the transition phase starts when the eNodeB receives a request from the Siesta. As described in the figure, $t_{on}$ holds the time from traffic active request to the time that the eNodeB completely reaches the active mode. $t_{off}$ means the duration from the sleep request to a complete sleep mode.

Now, we observe the number of message exchanges while the transition time $t_{on} + t_{off}$ for the eNodeB status changes. We assume that all messages provide the same

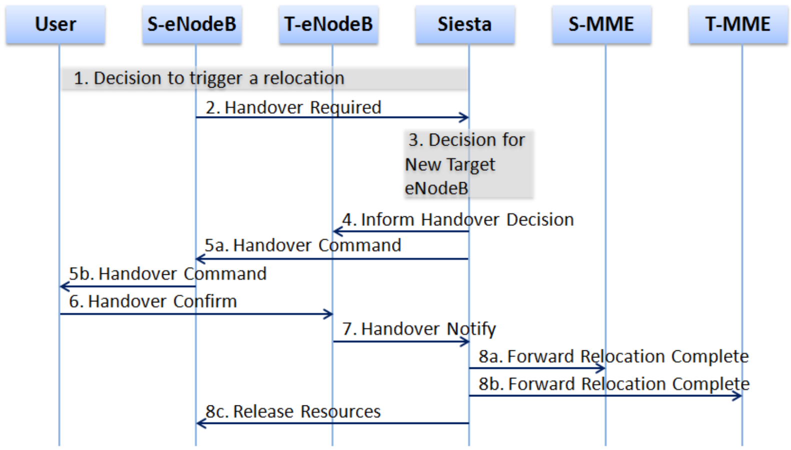


Figure 44: Handover procedure with Seista

overhead even if the message exchange occurs between different network elements. For example, the message between eNodeB and its neighbor and the message between Siesta and eNodeB are considered as the same. The number of control message exchange is described in Figure 43(b) by comparing previous schemes in Figure 42. Existing schemes show growth in the number of message exchanges while the number of neighboring eN-odeBs increase. Relax shows the most rapid increase because the number of users is considered in order to optimize the placement of the relay station. Here, relay stations are considered as eNodeBs, and the total number of users followed the example in [33] since we do not consider the number of users in analysis. Siesta shows the lowest number of message exchanges since the control messages are not exchanged between eNodeBs as described in Figure 42(d). Thus, Siesta isn't effected by the number of neighbor nodes.

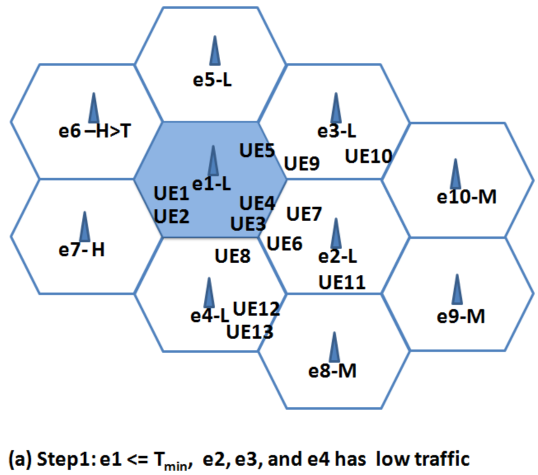


Figure 45: Scenario: Initial step

### 5.4.2 Handover Procedure with Siesta

The benefit of Siesta is also revealed in the handover procedure. Figure 44 illustrates the handover procedure in Siesta through the controller. Whenever the eNodeB encounters the threshold, Siesta decides whether the eNodeB changes the status or not. Suppose the decision is made to change the source-eNodeB (S-eNodeB) status. When Siesta sends the status change request to S-eNodeB, the users covered by S-eNodeB will receive the information. Then, the handover procedure starts.

The procedure can be described in three phases:

***Phase1: Inform decision to access network*** S-eNodeB sends the request message for a handover to Siesta. Siesta determines the new target eNodeB for each user and informs the handover decision to the target-eNodeB (T-eNodeB).

***Phase2: Handover between S-eNodeB and T-eNodeB*** The handover command transfer to the user through the S-eNodeB and the user will response to the T-eNodeB with a

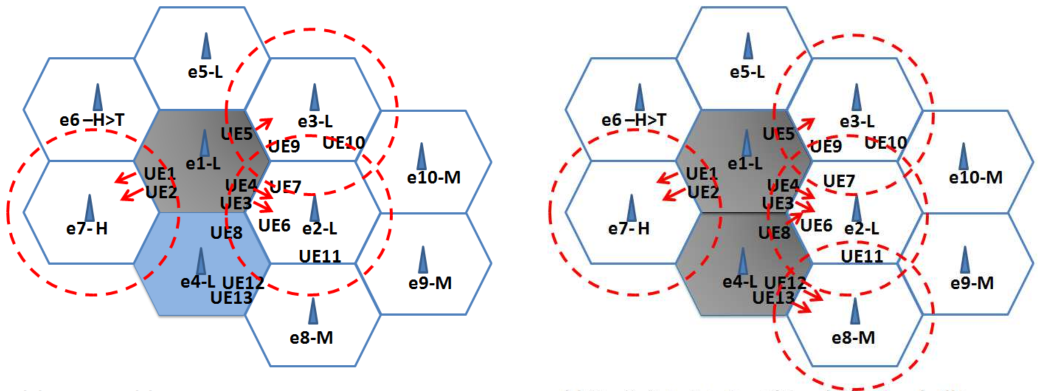


(b) Step2: Decision on e1 to sleep and e2, e3, and e7 increase, Consider e4 that has low traffic

(c) Step3: Calculate $P_1$ = P(sleep(e1) + sleep(e4)) + P(increase(e7) + increase(e2) + increase(e3) + increase(e8))

Figure 46: Scenario without centralized view

confirmation message. The T-eNodeB notifies handover to Siesta.

***Phase3: Report handover completion to the core network elements*** Siesta will forward the relocation complete message to both source MME and target MME while allowing the resource release from the S-eNodeB.

Compare to the traditional LTE handover procedure [74], the total number of message exchange is reduced and the message to MME is significantly decreased.

#### 5.4.3 Energy Saving Scenario

The global view of Siesta enables selecting the minimum set of active eNodeBs. Figure 47 illustrates the scenario that information beyond the neighbors empowers a reduction in the total energy consumption.

Suppose $e_1$, $e_2$, $e_3$, and $e_4$ has low traffic with a nighttime traffic decrease. The $e_5$ also has low traffic and $e_6$ and $e_7$ have high traffic and $e_6$ cannot support more users.

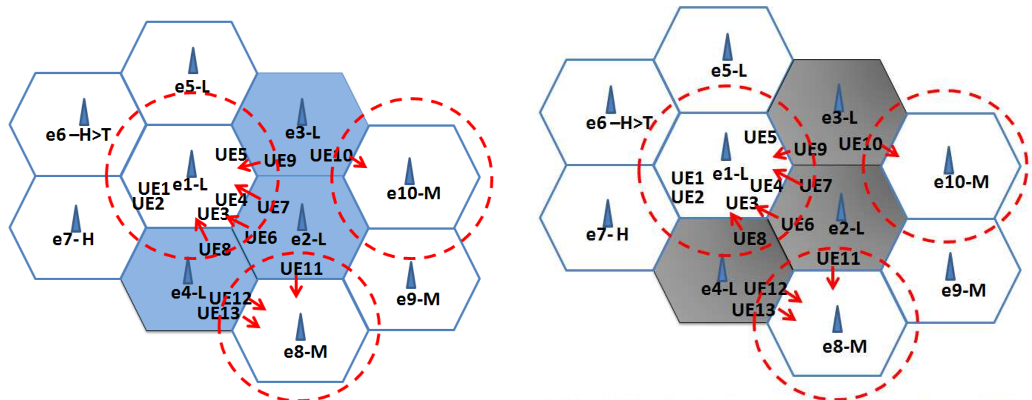


(b) Step2: Calculate $P_2$ = P(sleep(e2) + sleep(e3) + sleep(e4)) + P(increase(e1)+ increase(e8) + increase(e10))

(c) Step3: $P_1 > P_2$, Decision e2, e3, and e4 to sleep and e1, e8, and e10 increase

Figure 47: Energy saving scenario with Siesta

The $e_8$, $e_9$, and $e_{10}$ have medium traffic. Note that the users are described as $UE$ in Figure 46(a), and the users will be supported by the eNodeB which provides higher signal strength.

Let's assume $e_1$ reaches a minimum threshold with lowest traffic and the traffic of $e_2$, $e_3$, and $e_4$ is close to the minimum threshold as described in Figure 46(a). Then as illustrated in Figure 47(b) Siesta will calculate power consumption $P_1$ with the expected cell operation algorithm to reselect eNodeBs. $P_1$ includes the sleep mode energy consumption of $e_1$ and the increased mode of $e_2$, $e_3$, and $e_7$. In terms of handover, $UE_1$ and $UE_2$ are covered by $e_7$, $UE_3$ and $UE_4$ are covered by $e_2$, and $UE_5$ is covered by $e_3$. However, Siesta considers beyond the neighbors' status as illustrated in Figure 47. Siesta knows that $e_2$, $e_3$, and $e_4$ are close to the minimum threshold with low traffic and $e_8$, $e_9$, and $e_{10}$ can support the users from $e_2$, $e_3$, and $e_4$, as well. If all of users under $e_2$, $e_3$, and $e_4$ can be covered by other eNodeBs, Siesta calculates power consumption $P_2$ for $e_2$, $e_3$,

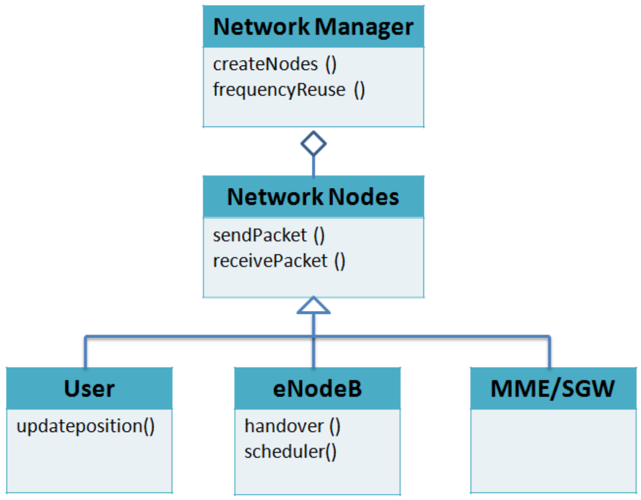


Figure 48: Architecture of LTE-Sim (Current LTE networks)

and $e_4$ sleep. Finally, Siesta compares the power consumption $P_1$ and $P_2$, then makes the decision to sleep $e_2$, $e_3$, and $e_4$ since $P_2$ is smaller than $P_1$ as shown in Figure 47(c).

Here, if Siesta does not consider the neighbors' status of $e_1$ then $e_1$ will go to sleep and other neighbors need to stay in active mode with increased traffic to take care of the users from $e_1$. However, with a global view of the network, some eNodeBs stay in active mode if they have a possibility to make more eNodeBs sleep. Moreover, $e_5$ gains a greater possibility for the sleep mode by increasing the power of $e_1$.

### 5.5 Evaluations with LTE Simulator

We have conducted evaluations to assess the performance of Siesta cell operation algorithm using a simulator called LTE-Sim [62] as well as trace-driven simulation. With LTE-sim, we have compared Siesta with current LTE network. Also, performance of Siesta is compared with a existing distributed algorithm [60] that is a representative sleep

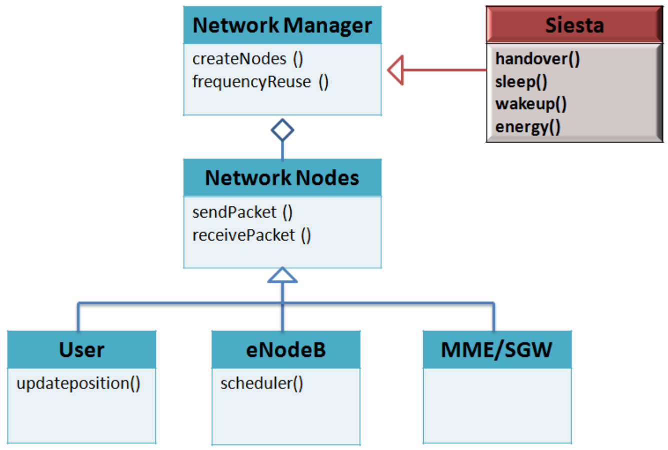


Figure 49: Architecture of SD-LTE-Sim (LTE-Sim with SDN architecture and Siesta)

and wake-up algorithm among various distributed control algorithms.

In order to compare the performance of Siesta cell operation algorithm with current LTE network, we have used a LTE network simulator named LTE-Sim. The simulator is a open source framework to simulate LTE networks and supports multi-cell environments, user mobility, handover procedures and frequency reuse techniques. As described in Figure 48, three network nodes are modeled: UE, eNodeB, and MME/GW. The networks nodes are controlled by one of the main components *NetworkManager*.

Table 7: Simulator Setting

| Parameter | Value |
|---|---|
| Cells | Macro cells (varied) |
| User mobility model | Random direction |
| Duplex mode | Frequency division duplex (FDD) |
| Scheduler | Proportional fair (PF) |
| Delay | 0.1 ms |

The *NetworkManager* also handles the users handover procedure and updates

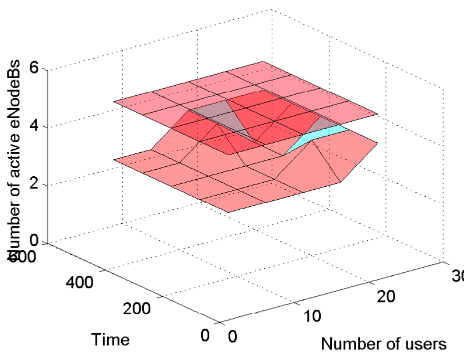


(a) Varied number of users

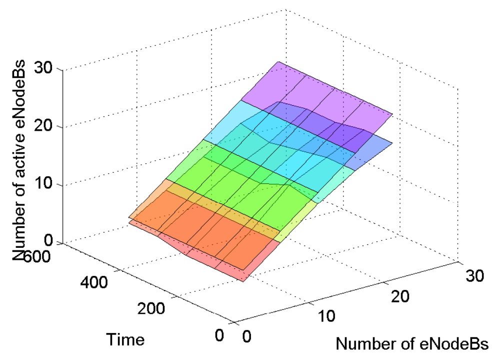


(b) Varied number of eNodeBs

Figure 50: Average number of active BS/eNodeBs (Upper surface: LTE-Sim with sleep/wakeup, Lower surface: SD-LTE-Sim)

users position. The random direction mobility model is used to simulate users' mobility. The handover decisions for each user are carried out by handover manager and performs based on the signal strength. More detailed simulation setting is shown in Table 7. For simulation, we have extended LTE-Sim. Figure 48 illustrates that handover decision is made by eNodeBs in current LTE network. We implemented Siesta on LTE-Sim at the *NetworkManager* level and named *SD-LTE-Sim* to provide global view of the network. The operations for sleep, wakeup, and handover is now controlled by Siesta as described in Figure 49. Additionally, energy saving based on eNodeB sleep/wakeup and users' handover is monitored and controlled by *SD-LTE-Sim*. While observing the performance of Siesta, LTE-Sim that presents current cellular network and *SD-LTE-Sim* are compared.

First, we observed the number of active eNodeBs with varied number of eNodeBs and varied number of users under each eNodeB over time. Figure 50(a) shows the results with varied number of eNodeBs with fixed number of users per eNodeB over time. Here,

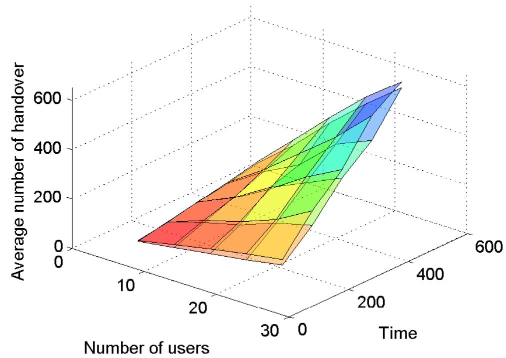


(a) Varied number of users

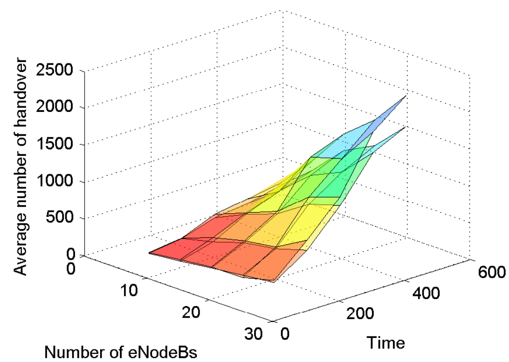


(b) Varied number of eNodeBs

Figure 51: Average number of handover (Upper surface: LTE-Sim with sleep/wakeup, Lower surface: SD-LTE-Sim)

we observe less number of active eNodeBs from *SD-LTE-Sim* since we have global view of the network. In Figure 50(b) that varies number of eNodeBs, we also observe more reduced number of active eNodeBs while we increase the number of eNodeBs in *SD-LTE-Sim*. From this result, we found that Siesta produces better operation for larger area coverage.

Next, the number of handover is observed over time with varied number of users and varied number of eNodeBs. From both results from varied number of users and eNodeBs, we found the reduced number of handover with *SD-LTE-Sim* as illustrated in Figure 51. Additionally, the number of handover reduces more while the size of the network increases.

Finally, the total energy consumption is considered with different size of the network and users. The Figure 52 presents that *SD-LTE-Sim* saves energy compare to the simple sleep/wakeup scheme.

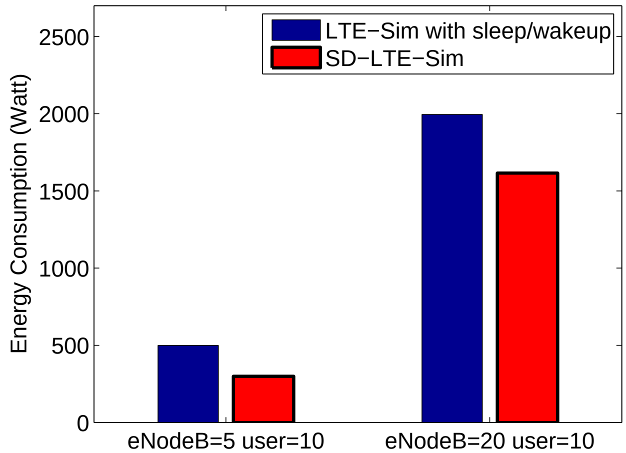


Figure 52: Comparison of total energy consumption between LTE-Sim (with sleep/wakeup) and SD-LTE-Sim (Designated number of user under each eNodeB)

With LTE simulator, LTE-Sim, we found that Siesta provides better control on the eNodeB status and users' handover so that we can save energy on the network.

### 5.6 Evaluations with Trace-Driven Simulation Results

We have evaluated the performance of our energy-aware cell operation algorithm on the larger size of the network and to observe the status of the network with real traces of human movement collected from 3 different sites. We consider the users move around in a $20^2$ $km$ area that can be representative of a large campus or city and eNodeBs are placed in a grid manner. The base eNodeB coverage range in the evaluation has a 1 $km$ radius as a macro eNodeB. Specific power consumption and transition time of an on-and-off mode follows [1].

For user movement data, we used real trace [7] from three sites: New York, Orlando, and NCSU. The total duration of user mobility is 12 hours and the interval of

Table 8: Data sets used (Real traces)

| Trace Site | New York | Orlando | NCSU |
|---|---|---|---|
| Number of users | 39 | 41 | 35 |
| Total visited cells | 72 cells | 30 cells | 45 cells |

location information is 30 seconds. The number of users is 39 in New York, 41 in Orlando, and 35 in NCSU. The total number of visited cells for each site is 72 cells in New York, 30 cells in Orlando, and 45 cells in NCSU. Since the number of users of the traces is relatively small, we assume all cells are initially active with the same level of static users in each cell. The number of users and the total number of visited cells for each site are described in Table 8. Since the number of users of the traces is relatively small, we assume all cells are initially active with the same level of static users in each cell. Then, user mobility is introduced from the human mobility traces creating dynamics of each cell.

We have conducted evaluations of our energy-aware cell operation algorithm and have compared its performance with a distributed algorithm that is a representative sleep and wake-up algorithm among various distributed control algorithms. In this algorithm, every active eNodeB makes its own decision independently.

We first observe the effectiveness of Siesta in terms of cell energy saving. We monitored the eNodeB sleep and awake status over time and compared the difference between a distributed algorithm and Siesta. Here, we present the results for the New York trace only due to space limitations. However, other traces exhibit similar patterns. In Figures 53 and 54, a yellow cell means that its cell range is increased, a green cell

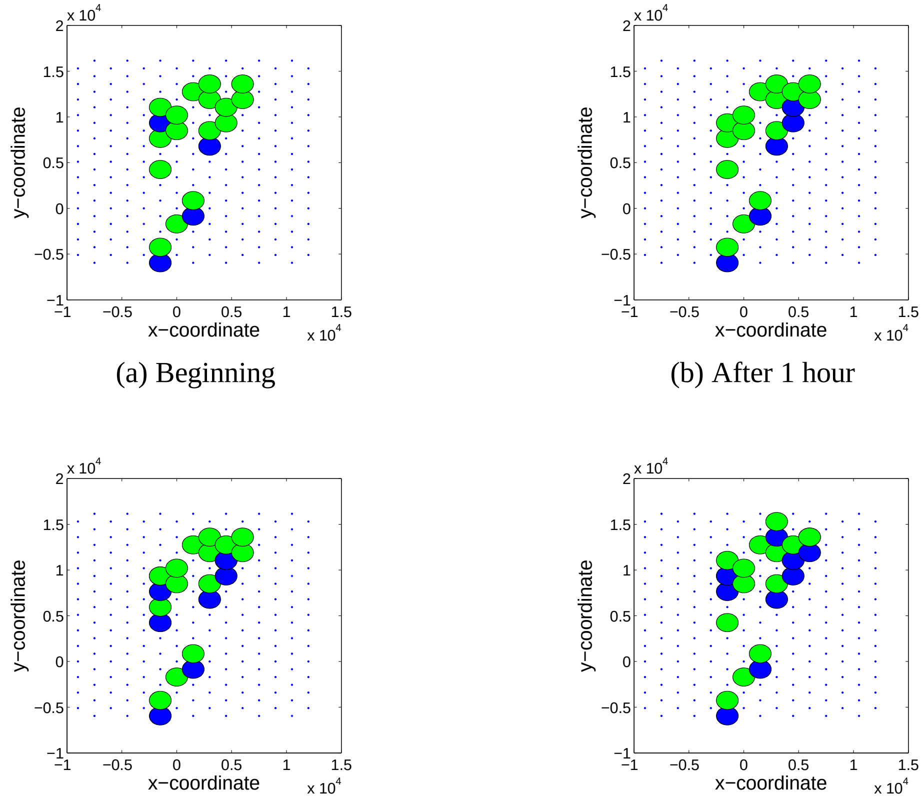


(a) Beginning (b) After 1 hour

(c) After 2 hours (d) After 3 hours

Figure 53: eNodeB sleep and awake status over time with a distributed algorithm

indicates that the eNodeB is active, and a blue cell denotes that the eNodeB is in sleep mode. In the comparison between Figure 53 and Figure 54, it is clearly observed that Siesta enables more eNodeBs to be in a sleep mode and less to be active while covering all the same users. By intelligently increasing a few eNodeBs' cell coverage, the neighboring cells find a greater possibility to sleep. The results with sector-based algorithm is shown in Figure 55

We now directly measure and compare the energy efficiency with respect to the achieved sleep time, the time spent in state transitions, and the total energy consumption

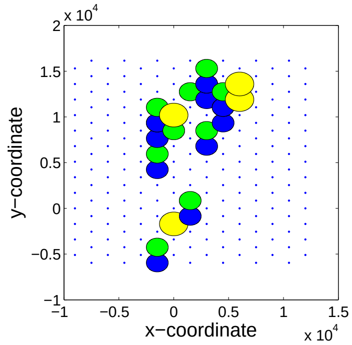


(a) Beginning

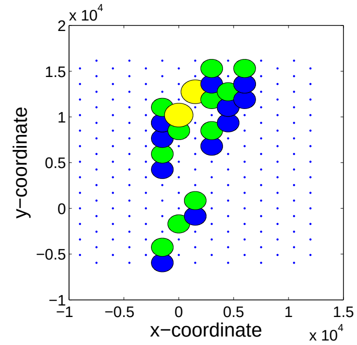


(b) After 1 hour

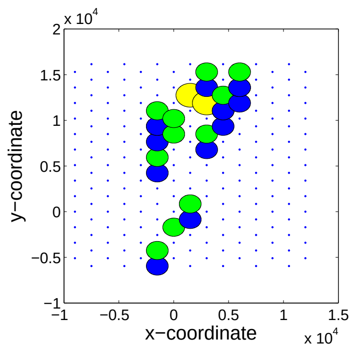


(c) After 2 hours

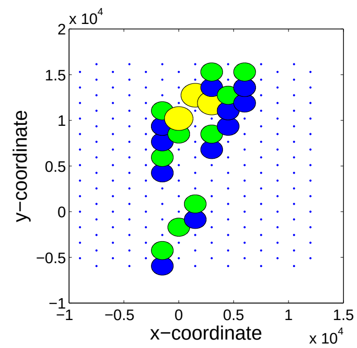


(d) After 3 hours

Figure 54: eNodeB sleep and awake status over time with Siesta - more sleep eNodeBs are achieved saving energy

of the network. We compared the sleep durations in each hour of data where the sleep duration for most of the eNodeBs with Siesta is longer than the distributed cell-zooming algorithm. The longer sleep instances also lead to less eNodeB mode transitions and lower energy consumption.

Figure 56 shows the cumulative state transition time where the value for each transition time between modes is set as $17 \mu s$ following [1], and the transition includes all changes to reach the new state such as active to sleep or active to increase. The cumulative transition time exposes the longer sleep instances without frequent status changes that

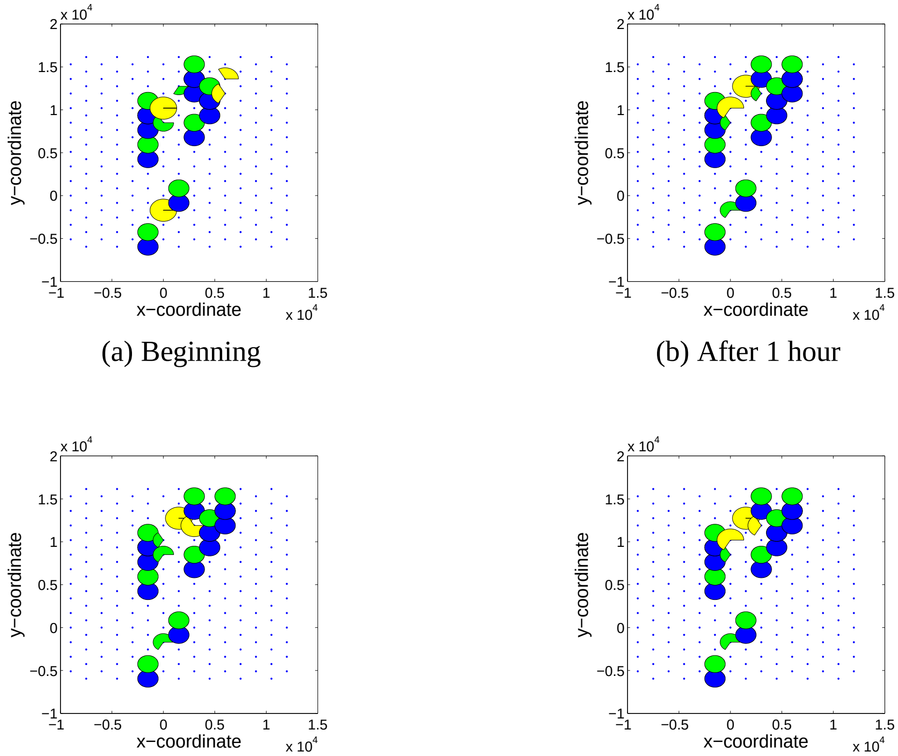


(a) Beginning

(b) After 1 hour

(c) After 2 hours

(d) After 3 hours

Figure 55: eNodeB sector-based sleep and awake status over time with Siesta

indicate the stability in the network operation and energy saving. Figure 57 depicts that the number of handovers also decreased with Siesta. This reduced number of handovers correlates closely with the reduced number on mode changes. With this reduced status change rate, eNodeB can stay in the sleep mode longer. The total energy consumption is shown in Figure 58 comparing Siesta with the one without sleep and awake scheme and the distributed cell-zooming scheme. The energy consumption of Siesta is clearly the lowest with all three traces.

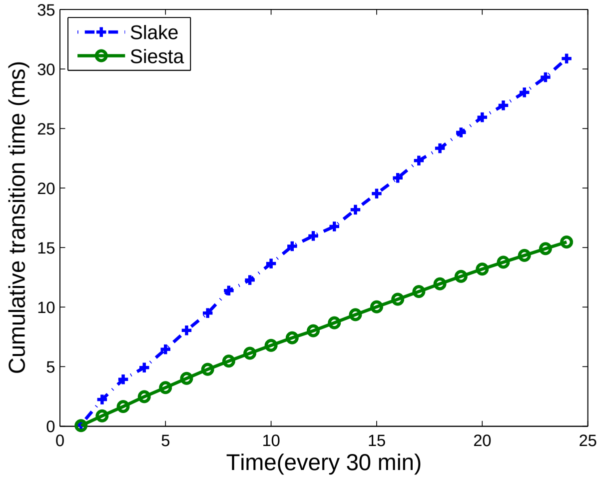


Figure 56: Comparison of eNodeB benefits over time on transition time

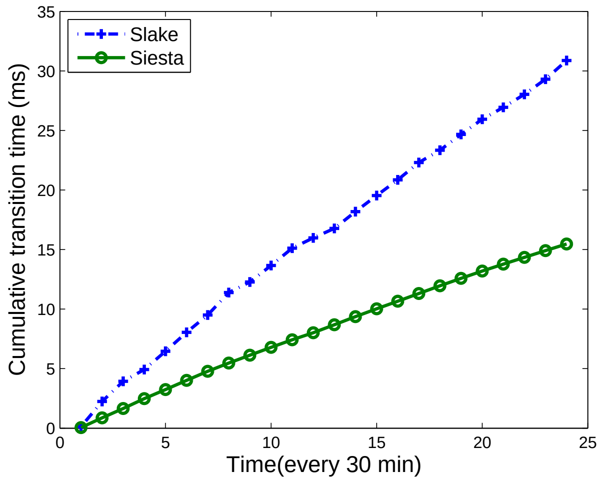


Figure 57: Comparison of eNodeB benefits over time on number of handovers

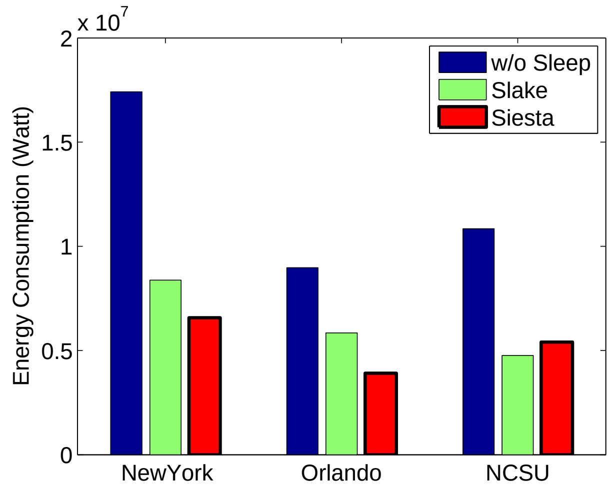


Figure 58: Comparison of energy saving

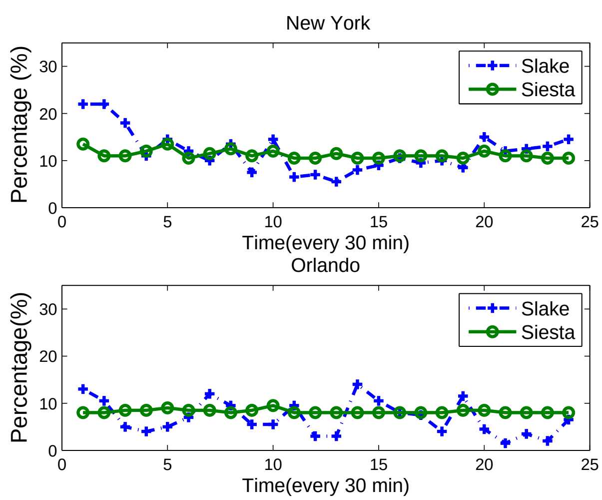


Figure 59: Comparison of eNodeB status stability over time with % of Sleep eNodeBs

Table 9: Coefficient of variation of the number of sleep eNodeBs

| | New York | Orlando | NCSU |
|---|---|---|---|
| Distributed | 36.6251 | 52.6345 | 43.0649 |
| Siesta | 10.2225 | 6.7843 | 6.1734 |

Next, we evaluate the variations of eNodeB status changes for eNodeB status stability. A smaller variation in eNodeB's on-and-off status change indicates a lower probability of the ping-pong effect that is a well-known problem in cellular networks. The ping-pong effect can increase the energy consumption with frequent on-and-off of eNodeBs. It also causes frequent handovers that increase control messages to the core network and decrease the users' QoS. Table 9 shows the coefficient of variation on the number of asleep eNodeBs, and Siesta is far more stable than a distributed cell-zooming approach. To investigate the performance of Siesta in detail, the percentage of asleep eNodeBs over time is shown in Figure 59. The percentage of sleep eNodeBs prominently fluctuates in a distributed cell-zooming scheme. Meanwhile, Siesta displays a stable behavior over time, as the virtualized cell management function uses a global view of the network and selects the cells to be active where more users reside. That is, the cells considered as hot spots will be in an increased or active mode. Moreover, the number of eNodeB status changes in Figure 60 also shows in a smaller number and in stable change rate with Siesta.

In summary, the proposed Siesta leads to a greater number of eNodeBs in sleep and for a longer duration than a state-of-the-art cell-zooming algorithm. Siesta also yields greater status stability as well as energy savings for the whole cellular network.

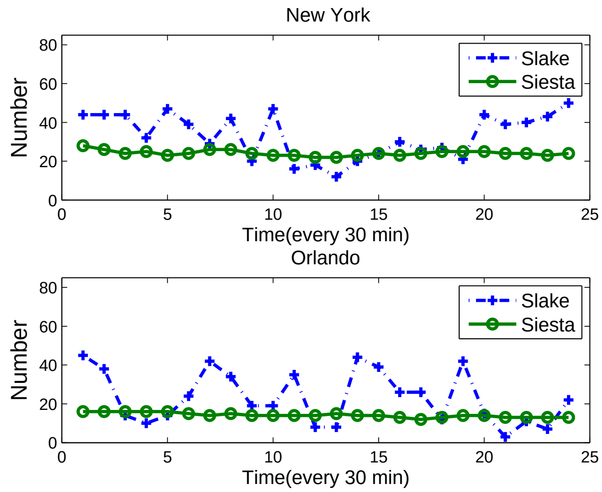


Figure 60: Comparison of eNodeB status stability over time with eNodeB status change

### 5.7 Summary

We have proposed Siesta (Software-defined energy efficient base station control) that is a novel NFV of the cell management communicate with SDN controler. Siesta provides significant benefits over the current cellular networks that suffer from inflexible management and complex control. Through the eNodeB power control architecture and the proposed algorithm, Siesta greatly improves energy efficiency in a cellular network yielding the higher number of eNodeBs in a sleep mode as well as the longer sleep durations compared with other existing energy efficient techniques. The cell management architecture and procedure also greatly simplify the control over the sleep and awake modes of eNodeBs and enable an agile handover operations. Siesta exhibits desirable operational features of stability such as less control message exchanges, less eNodeB status changes, and less handovers. We have validated the results through both LTE cellular network simulator that improved with SDN architecture and extensive trace-driven evaluations for observation on the larger network.

# CHAPTER 6

# SUMMARY

The ubiquity of mobile telephony is rapidly expanding, especially with the popularity of smartphones in recent years. As data traffic and the number of subscribers increase, there are a number of different challenges and requirements the mobile network need to e able to handle. Moreover, the expectation on quality and services brings more challenges to cellular operators and make cellular networks keep evolving. The agility, flexibility, and manageability of the network can be achieved with SDN and NFV in cellular networks. This dissertation specifically focused on functionality of location management and energy efficiency in cellular systems that can be virtualized. Furthermore, SDN gives a centralized view of the network and brings better results.

First of all, we proposed a group location management scheme as a virtualized network function in cellular networks for an improved group application service. The presence of the virtualized group management function efficiently facilitates the group location management task and enables a provider to handle a large number of members and groups that otherwise would be impossible in practice. The group profiling algorithm dynamically updates its group members' locations information with clusters of cells or tracking areas that can be of arbitrary shapes. We validated the efficiency of the proposed scheme with theoretical analyses as well as experiments. The theoretical analyses showed the total signaling traffic cost and significant reduction of average delay. As for the experiments, we used both real traces of human movements and synthetic human mobility data for the tracking area update and paging costs. Moreover, we investigated the impact of the parameter that describes the self-similarity of the human walk and suggested the range of the threshold that decides the size of the TA. To the best of our knowledge, our work is the first to address the issue of location management for group applications.

For the location management, there are related challenges that need to be addressed in the future. The benefit of the proposed architecture can be further substantiated with the development and evaluation of a group call signaling protocol that we plan to address in the near future. Also, there is no human group mobility model at the moment, and it would be useful for evaluations of schemes for group applications. That will also enable us to perform a detailed theoretical analysis of the proposed group location management scheme.

Secondly, we have proposed Siesta (Software-defined energy efficient base station control) that is a novel network function virtualization (NFV) of the cell management. Siesta provides significant benefits over the current cellular networks that suffer from inflexible management and complex control. Through the eNodeB power control architecture and the proposed algorithm, Siesta greatly improves energy efficiency in a cellular network yielding the higher number of eNodeBs in a sleep mode as well as the longer sleep durations compared with other existing energy efficient techniques. The cell management architecture and procedure also greatly simplify the control over the sleep and awake modes of eNodeBs and enable an agile handover operations. Siesta exhibits desirable operational features of stability such as less control message exchanges, less eNodeB status changes, and less handovers. We have validated the results through extensive trace-driven evaluations.

# CHAPTER 7

# FUTURE WORK

Mobile access networks will experience significant challenges on data rates, user coverage in hot spots with low latency, and energy consumption. The number of subscriptions exceeds the population in many countries and expect to reach 7.7 billion globally by 2021 [30]. Also, the Internet of Things (IoT) is contributing to increase mobile traffic with smart devices and wearable devices. To address challenges, 5G has already emerged as a key method regarding the expanded connectivity and targeting commercialization in 2020.

The challenges and requirements for 5G mobile systems are outlined as follows [39].

- Data rate and latency: 5G networks are envisioned to enable an experienced data rate of 300 Mbps and 60 Mbps in downlink and uplink, respectively.

- Multiple radio access technologies: Existing RAN, including GSM, HSPA+, and LTE will continue to evolve to provide a superior system performance.

- Network-assisted Device-to-device(D2D) communication: D2D communication in cellular networks is defined as direct communication between two mobile users without traversing the BS or core network.

- Energy-efficient communication: Improve the energy efficiency of the battery constrained wireless devices.

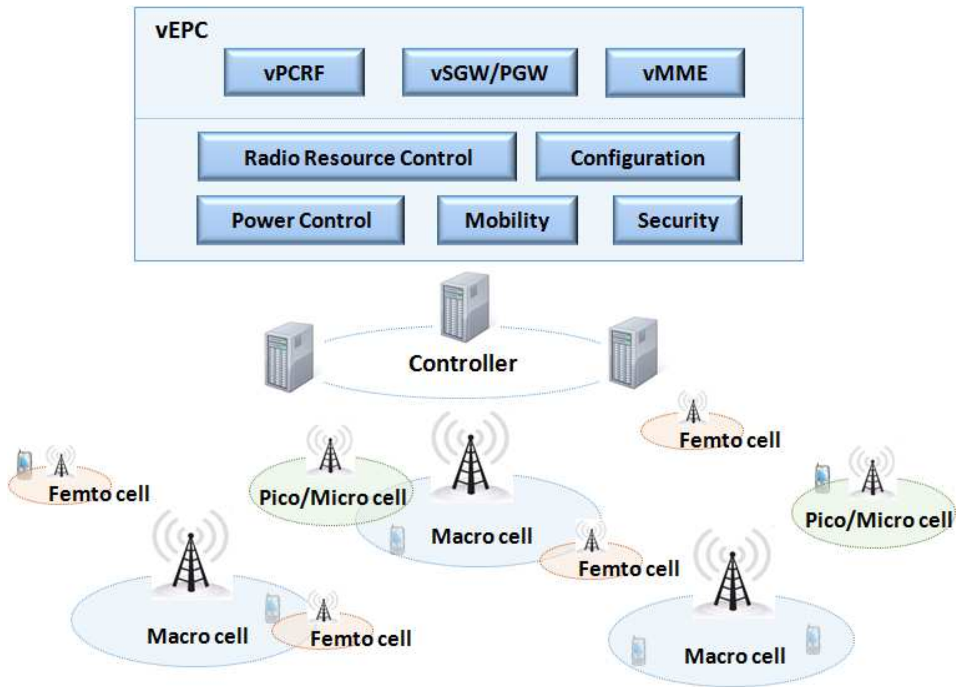


Figure 61: Architecture of future cellular networks

In detail, D2D communications was initially proposed in cellular networks as a new paradigm for enhancing network performance. The emergence of new applications such as content distribution and location-aware advertisement introduced new user cases for D2D communications in cellular networks [15].

Furthermore, one of the main challenges in future wireless networks is to improve the energy efficiency. A study estimating the energy consumed by mobile networks in Sweden shows that over the past 6 years, data traffic increased over 13 times while energy consumption grew by around 40 percent [30].

Based on our studies and the challenges of future networks, further development can be continued on the virtualizing control functions of eNodeB. As described in Figure 61, radio resource control, configuration, and security also can be developed as VNFs.

This can simplify the role of eNodeBs in the network and provide flexibility on management. In addition, we also can extend and improve our work with user-centric concept for heterogeneous deployment on RAN. For example, the eNodeB control can be done based on users' needs. Our current work shows that eNodeBs are active and perform sleep and wakeup based on current traffic. However, eNodeB can be turned on whenever users' needs exist with user-centric concept. VNF of power control can handle various size of eNodeBs such as macro cell, pico/micro cell and femto cell with global view of the network and offer energy saving and better QoS to users.

## REFERENCE LIST

[1] Agilent Technologies. http://www.chem.agilent.com.

[2] AT&T Enhanced Push to Talk. http://www.corp.att.com/.

[3] GreenTouch Consortium. http://http://www.greentouch.org.

[4] Nextel Direct Connect . http://www.sprint.com/.

[5] Open Mobile Alliance. http://www.openmobilealliance.org/.

[6] Verizon Wireless – Push to Talk. http://www.verisonwireless.com/.

[7] A Community Resource for Archiving Wireless Data At Dartmouth (CRAWDAD). http://crawdad.cs.dartmouth.edu/data.php.

[8] Adly, N., and El-Nahas, A. A Profile-Based Hierarchical Location Management Scheme for Future PCS. In *Proc. 11th Int. Workshop Database and Expert Systems Applications (DEXA)* (2000), pp. 204 – 208.

[9] Akyildiz, I. F., Gutierrez-Estevez, D. M., and Reyes, E. C. The Evolution to 4G Cellular Systems: LTE-Advanced. *Phys. Commun. 3*, 4 (December 2010), 217–244.

[10] Alcatel-Lucent. Introduction to Evolved Packet core. Tech. rep., March 2009.

[11] Alcatel-Lucent. The Journey to Packet Core Virtualization: Evolving the Packet core to an NFV/SDN Architecture. Tech. rep., 2014.

[12] Alcatel-Lucent. The Journey to Packet Core Virtualization: Evolving the Packet Core to an NFV/SDN Architecture. Tech. rep., February 2014.

[13] Americas, G. The benefits of SON in LTE: Self-optimizing and self-organizing networks. Tech. rep., December 2009.

[14] Arnold, O., Richter, F., Fettweis, G., and Blume, O. Power Consumption Modeling of Different Base Station Types in Heterogeneous Cellular Networks. In *Future Network and Mobile Summit* (June 2010), pp. 1–8.

[15] Asadi, A., Wang, Q., and Mancuso, V. A Survey on Device-to-Device Communication in Cellular Networks. *Communications Surveys Tutorials, IEEE 16*, 4 (2014), 1801–1819.

[16] Auer, G., and et al. D2.3 v2 : Energy efficiency analysis of the reference systems, areas of improvement and target breakdown. Tech. rep., INFSO-ICT-247733 EARTH (Energy Aware Radio and NeTwork TecHnologies), 2012.

[17] Bar-Noy, A., Kessler, I., and Sidi, M. Mobile Users: to Update or Not to Update? In *IEEE Proc. 13th Networking for Global Communications (INFOCOM)* (1994).

[18] Basta, A., Kellerer, W., Hoffmann, M., Hoffmann, K., and Schmidt, E.-D. A Virtual SDN-Enabled LTE EPC Architecture: A Case Study for S-/P-Gateways Functions. In *Future Networks and Services (SDN4FNS), IEEE SDN for* (2013).

[19] Benzaid, C., and Badache, N. A Causal Multicast Protocol for Dynamic Groups in Cellular Networks. In *Proc. Euro American Conf. Telematics and Information Systems (EATIS)* (2008).

[20] Bhaumik, S., Narlikar, G., Chattopadhyay, S., and Kanugovi, S. Breathe to stay cool: adjusting cell sizes to reduce energy consumption. In *Proceedings of the first ACM SIGCOMM workshop on Green networking* (2010), Green Networking, pp. 41–46.

[21] Bousia, A, A. A., Alonso, L., and Verikoukis, C. Green Distance-aware Base Station Sleeping Algorithm in LTE-Advanced. In *Communications (ICC),IEEE International Conference on* (June 2012), pp. 1347–1351.

[22] Cayirci, E., and Akyildiz, I. Optimal Location Area Design to Minimize Registration Signaling Traffic in Wireless Systems. *IEEE Trans. Mobile Computing* (2003).

[23] Chen, J.-L., and Wang, K.-C. Reliable WiMAX Multicast Applications. In *Proc. IEEE 8th Int. Conf. Computer and Information Technology Workshops* (2008), pp. 182 – 187.

[24] Chiang, K.-H., and Shenoy, N. Performance of an Overlapped Macro-cell Based Location Area Scheme. In *IEEE Int. Conf. Communications (ICC)* (2003).

[25] Chvatal, V. A Greedy Heuristic for the Set-Covering Problem. *Mathematics of Operations Research 4*, 3 (1979), 233–235.

[26] Claussen, H., Ho, L. T. W., and Pivit, F. Effects of joint macrocell and residential picocell deployment on the network energy efficiency. In *Personal, Indoor and Mobile Radio Communications (PIMRC) IEEE 19th International Symposium on* (September 2008), pp. 1–6.

[27] Committee, O. M. E. Software-defined Networking: The New Norm for Networks, April 2012.

[28] Communication, F. N. The Benefits of Cloud-RAN Architecture in Mobile Network Expansion. Tech. rep., 2014.

[29] Elayoubi, S.-E., Saker, L., and Chahed, T. Optimal control for base station sleep mode in energy efficient radio access networks. In *INFOCOM, Proceedings IEEE* (April 2011), pp. 106–110.

[30] Ericsson. Ericsson Mobility Report on the Pulse of the Networked Society. Tech. rep., November 2015.

[31] Ester, M., Kriegel, H., Sander, J., and Xu, X. A Density-Based Algorithm for Discovering Clusters in Large Spatial Databases with Noise. In *Proc. 2nd Int. Conf. Knowledge Discovery and Data mining* (1996), pp. 226 – 231.

[32] (ETSI), E. T. S. I. Network Function Virtualization - An Introduction, Benefits, Enablers, Challenges and Call for Action. Tech. rep., October 2012.

[33] Gao, C., Zhang, W., Tang, J., Wang, C., Zou, S., and Su, S. Relax, but Do Not Sleep: A new perspective on Green Wireless Networking. In *INFOCOM, Proceedings IEEE* (April 2014), pp. 907–915.

[34] Gomez, K., Rasheed, T., Reynaud, L., and Goratti, L. FME: A Flexible Management Entity for virtualizing LTE Evolved Packet Core. In *Network Operations and Management Symposium (NOMS),IEEE* (2014).

[35] Gudipati, A., Perry, D., Li, L. E., and Katti, S. SoftRAN: Software Defined Radio Access Network. In *Proceedings of the Second ACM SIGCOMM Workshop on Hot Topics in Software Defined Networking (HotSDN)* (2013), pp. 25–30.

[36] Haberland, B., Derakhshan, F., Grob-Lipski, H., Klotsche, R., Rehm, W., Schefczik, P., and Soellner, M. Radio Base Stations in the Cloud. *Bell Labs Technical Journal 18*, 1 (June 2013), 129–152.

[37] Han, C., Harrold, T., Armour, S., Krikidis, I., Videv, S., Grant, P., Haas, H., Thompson, J., Ku, I., Wang, C.-X., Le, T. A., Nakhai, M., Zhang, J., and Hanzo, L. Green radio: radio techniques to enable energy-efficient wireless networks. *Communications Magazine, IEEE 49*, 6 (June 2011), 46–54.

[38] Han, I., and Cho, D.-H. Group Location Management for Transportation Systems in Wireless Cellular Systems. In *IEEE 54th Vehicular Technology Conf. (VTC)* (2001), vol. 4, pp. 2726 – 2730.

[39] Hossain, E., Rasti, M., Tabassum, H., and Abdelnasser, A. Evolution toward 5G multi-tier cellular wireless networks: An interference management perspective. *Wireless Communications, IEEE 21*, 3 (June 2014), 118–127.

[40] Hossain, M., Munasinghe, K., and Jamalipour, A. A protocooperation-based sleep-wake architecture for next generation green cellular access networks. In *Signal Processing and Communication Systems (ICSPCS), 4th International Conference on* (December 2010), pp. 1–8.

[41] I, C.-L., Huang, J., Duan, R., Cui, C., Jiang, J., and Li, L. Recent Progress on C-RAN Centralization and Cloudification. *Access, IEEE 2* (2014), 1030–1039.

[42] Inc., T. I. LTE in a Nutshell: Protocol Architectur. Tech. rep., 2010.

[43] Jin, X., Li, L. E., Vanbever, L., and Rexford, J. SoftCell: Scalable and Flexible Cellular Core Network Architecture. In *Proceedings of the Ninth ACM Conference on Emerging Networking Experiments and Technologies (CoNEXT)* (2013), pp. 163–174.

[44] Kelif, J. M., Coupechoux, M., and Marache, F. Limiting Power Transmission of Green Cellular Networks: Impact on Coverage and Capacity. In *ICC* (2010), pp. 1–6.

[45] Lam, G. H. K., Leong, H. V., and Chan, S. C. F. Reducing Group Management Overhead in Group-Based Location Management. In *Proc. 15th Int. Workshop Database and Expert Systems Applications* (2004), pp. 640 – 644.

[46] Lee, D. C., jin Kim, H., Lee, J., and Lin, Y. B. Performance Analysis of the Distributed Location Management Scheme in Large Mobile Networks. *Journal of Information Processing Systems 1*, 1 (2005), 55 – 61.

[47] Lee, K., Hong, S., Kim, S. J., Rhee, I., and Chong, S. SLAW: A New Mobility Model for Human Walks. In *Proc IEEE INFOCOM* (2009), pp. 855 – 863.

[48] Li Erran Li, Z. M. M., and Rexford, J. Toward software-defined cellular networks. In *Proc. European Workshop on Software Defined Networking (EWSDN)* (October 2012).

[49] Lin, Y. Reducing Location Update Cost in a PCS Network. *IEEE/ACM Trans. Networking 5*, 1 (1997), 25 – 33.

[50] Liou, R.-H., Lin, Y.-B., and Tsai, S.-C. An Investigation on LTE Mobility Management. *Mobile Computing, IEEE Transactions on* (2013).

[51] Liu, J., Sacchetti, D., Sailhan, F., and Issarny, V. Group Management for Mobile Ad Hoc Networks: Design, Implementation and Experiment. In *Proc. 6th Int. Conf. Mobile Data Management (MDM)* (2005).

[52] Liyanage, M., Gurdrei, A., and Yilanttila, M. *Software Defined Mobile Networks - beyond LTE Network Architecture*. No. ISBN 978-1-118-90028-4. Wiley, 2015.

[53] Marsan, M. A., Chiaraviglio, L., Ciullo, D., and Meo, M. OptimalEnergy Savings in Cellular Access Networks. In *IEEE International Conference on Communications Workshops* (June 2009).

[54] Marsan, M. A., and Meo, M. Energy Efficient Wireless Internet Access with Cooperative Cellular Networks. In *Computer Networks* (2010).

[55] Mobile, C. C-RAN The Road Towards Green RAN. Tech. rep., October 2011.

[56] Morosi, S., Del Re, E., and Piunti, P. Traffic based energy saving strategies for green cellular networks. In *European Wireless, 18th European Wireless Conference* (April 2012), pp. 1–6.

[57] Networks, F. Network Functions Virtualization - Everything Old Is New Again. Tech. rep., 2013.

[58] Ng, C. K., and Chan, H. W. Enhanced Distance-Based Location Management of Mobile Communication Systems Using a Cell Coordinates Approach. *IEEE Trans. Mobile Computing 4*, 1.

[59] Niu, Z., Wu, Y., Gong, J., and Yang, Z. Cell zooming for cost-efficient green cellular networks. *Communications Magazine, IEEE 48*, 11 (November 2010), 74–79.

[60] Oh, E., Son, K., and Krishnamachari, B. Dynamic Base Station Switching-On/Off Strategies for Green Cellular Networks. *Wireless Communications, IEEE Transactions on 12*, 5 (May 2013), 2126–2136.

[61] Parija, S., Nanda, S., Sahu, P., and Singh, S. Novel Intelligent Soft Computing Techniques for Location Prediction in Mobility Management. In *Engineering and Systems (SCES), Students Conference on* (2013).

[62] Piro, G., Grieco, L., Boggia, G., Capozzi, F., and Camarda, P. Simulating LTE Cellular Systems: An Open-Source Framework. *Vehicular Technology, IEEE Transactions on 60*, 2 (February 2011), 498–513.

[63] Pollini, G., and I, C.-L. A Profile-Based Location Strategy and its Performance. *IEEE Journal on Selected Areas in Communications* (1997).

[64] Ratnam, K., Matta, I., and Rangarajan, S. A Fully Distributed Location Management Scheme for Large PCS Networks, 1999.

[65] Roy, A., Misra, A., and Das, S. K. Location Update versus Paging Trade-Off in Cellular Networks: An Approach Based on Vector Quantization. *IEEE Trans. Mobile Computing 6*, 12.

[66] Said, S. B. H., Guillouard, K., and Bonnin, J. On the benefit of context-awareness for security mechanisms in LTE/EPS networks. In *24th IEEE Annual International Symposium on Personal, Indoor, and Mobile Radio Communications, PIMRC, September, 2013* (2013).

[67] Saker, L., Elayoubi, S.-E., and Chahed, T. Minimizing Energy Consumption via Sleep Mode in Green Base Station. In *Wireless Communications and Networking Conference (WCNC), IEEE* (April 2010), pp. 1–6.

[68] Schmelz, L. C., Berg, J. V. D., Litjens, R., ICT, T., Zetterberg, K., and Amirijoo, M. Self-organisation in Wireless Networks Use Cases and their Interrelation. In *22nd Wireless World Research Forum (WWRF)* (May 2009).

[69] SDN, and Congress, O. W. Network Functions Virtualisation (NFV) - An Introduction, Benefits, Enablers, Challenges and Call for Action. Tech. rep.

[70] Simone Morosi, P. P., and Re, E. D. Sleep Mode Management in Cellular Networks: A Traffic Based Technique Enabling Energy Saving. *Transactions on Emerging Telecommunications Technologies 24*, 3 (2013), 331–341.

[71] Singh, J., and Karnan, M. Using a Novel Intelligent Location Management Strategy in Cellular Networks. In *Signal Acquisition and Processing ICSAP '10. International Conference on* (2010).

[72] Son, K., and Krishnamachari, B. SpeedBalance: Speed-scaling-aware optimal load balancing for green cellular networks. In *INFOCOM, Proceedings IEEE* (March 2012), pp. 2816–2820.

[73] Son, K., Oh, E., and Krishnamachari, B. Energy-aware hierarchical cell configuration: From deployment to operation. In *Computer Communications Workshops (INFOCOM WKSHPS),IEEE Conference on* (April 2011), pp. 289–294.

[74] Stefania Sesia, Issam Toufik, M. B. *LTE - The UMTS Long Term Evolution: From Theory to Practice*. No. ISBN 978-0-470-74288-4. Wiley, 2009.

[75] Tcha, D.-W., Choi, T.-J., and Myung, Y.-S. Location-Area Partitioning in a Cellular Radio Network. *The Journal of the Operational Research Society 48*, 11 (1997), 1076 – 1081.

[76] Varsamopoulos, G., and Gupta, S. Dynamically Adapting Registration Areas to User Mobility and Call Patterns for Efficient Location Management in PCS Networks. *IEEE/ACM Trans. Networking* (2004).

[77] Varsamopoulos, G., and Gupta, S. Optimal Offline and Online Registration Techniques for Location Management with Overlapping Registration Areas. *IEEE Trans. Mobile Computing* (2005).

[78] Verkama, M. A Simple Implementation of Distance-Based Location Updates. In *IEEE 6th Int. Conf. Universal Personal Communications Record* (1997).

[79] Wu, X., Mukherjee, B., and Bhargava, B. A Low-Cost, Low-Delay Location Update/Paging Scheme in Hierarchical Cellular Networks. In *Proceedings of the 3rd ACM International Workshop on Data Engineering for Wireless and Mobile Access* (2003), pp. 46 – 50.

[80] Wu, X., Mukherjee, B., and Bhargava, B. A Crossing-Tier Location Update/Paging Scheme in Hierarchical Cellular Networks. *IEEE Trans. Wireless Communications* (2006).

[81] Wuthnow, M., Stafford, M., and Shih, J. *IMS: A New Model for Blending Applications*. No. ISBN 1-4200-9285-5. Taylor and Francis, 2009.

# VITA

Sunae Shin was born in Seoul, South Korea, on October 11, 1981. Ms. Shin entered the Kyung Hee University in South Korea in March 2001 and graduated in July 2005 with a Bachelor of Engineering degree in Computer Engineering. After graduation, Ms. Shin came to the USA to study and gained a Master of Science degree in Computer Science from South Dakota State University at Brookings in South Dakota in December 2007. Her thesis topic was an enhanced retrieval tool for EJB components for components based software development.

After her Master degree, Ms. Shin joined interdisciplinary Ph.D. curriculum at the University of Missouri-Kansas City in 2008. Her coordinating discipline is Telecommunications and Computer Networking and her co-discipline is Electrical and Computer Engineering. Her main research interest and dissertation topic is base station control and mobility management with software-defined networking for green cellular networks. Ms. Shin also performed several distinct projects in various areas such as data transfer protocol using network testbeds, energy efficiency in wireless sensor networks, and smartphone-based collision avoidance system. Along with research, she have acquired teaching experiences. She taught Discrete mathematics I and Problem solving & programming lab at University of Missouri - Kansas City.

During her Ph.D. study, Ms. Shin received the first poster award from the Grace Hopper Celebration (GHC) regional conference - Missouri, Iowa, Nebraska, and Kansas Women in Computing (MINKWIC) conference in 2011. She also awarded scholarship of

Graduate Assistance Fund (GAF) through UMKC women′s council in 2013 and several travel grants from GENI Engineering Conference (GEC) in 2013 and Central Area Networking and Security workshop (CANSec) in 2014. Additionally, she received Outstanding Ph.D. student award from Telecommunication and Computer Networking discipline in 2014. She also gained research grant from University of Missouri - Kansas City, School of Graduate Studies Research award program in 2015.